Information Sciences 616 (2022) 255–275

Contents lists available at ScienceDirect

Information Sciences

journal homepage: www.elsevier.com/locate/ins

The bootstrap for testing the equality of two multivariate time series with an application to financial markets

Ángel López-Oriona *, José A. Vilar

Research Group MODES, Centre for Information and Communications Technology Research (CITIC), University of A Coruña, 15071 A Coruña, Spain

ARTICLE INFO

Article history:
Received 29 April 2022
Received in revised form 8 October 2022
Accepted 10 October 2022
Available online 17 October 2022

Keyword:
Multivariate time series
Quantile cross-spectral density
Frequency domain
Moving blocks bootstrap
Stationary bootstrap
Dotcom bubble

ABSTRACT

The problem of testing the equality of the generating processes of two multivariate time series is addressed in this work. To this aim, we construct four tests based on a distance measure between stochastic processes. The metric is defined in terms of the quantile cross-spectral densities of both processes. A proper estimate of this dissimilarity is the cornerstone of the proposed tests. The first test employs the asymptotic distribution of the estimate, which we derive from some standard results on complex random variables and which is useful in its own right. The bad behaviour of this test when compared with alternative ones is shown. The three remaining techniques are based on the bootstrap. Specifically, a particular bootstrap method for spectral densities and extensions of the moving blocks bootstrap and the stationary bootstrap are used for their construction. The approaches are assessed in a broad range of scenarios under the null and the alternative hypothesis. The results from the analyses show that the procedure based on the stationary bootstrap exhibits the best overall performance in terms of both size and power. The proposed techniques are used to answer the question about whether or not the dotcom bubble crash of 2000s permanently impacted the global market behavior.

1. Introduction

The problem of comparing two time series arises in a natural way in multiple fields, including machine learning, finance, computer science, biology, medicine, physics, biology, psychology, among others. For instance, an investor often has to determine if two particular assets show the same behavior over time based on historical data. In physics, it is usually interesting to find out to what extent ECG signals from different subjects exhibit similar patterns. A wide variety of data mining and statistical techniques have been proposed to address this kind of problems, including cluster analysis [1], classification [2], outlier detection [3], and comparisons through hypothesis tests [4]. It is worth highlighting that these techniques have mainly focused on univariate time series (UTS) [5–8], while the study of multivariate time series (MTS) has received less attention [9,10].

Frequently these techniques require to evaluate dissimilarity between time series, which is not a simple issue due to the dynamic character of these data objects. In fact, the problem of determining a suitable dissimilarity measure between time series has become an important research topic during recent years. Lafuente-Rego and Vilar [6] provided a clustering algorithm for time series based on an innovative distance comparing the so-called quantile autocovariance functions. Other dissimilarity criteria recently proposed to construct fuzzy clustering procedures include distances between: estimated

* Corresponding author.
E-mail addresses: oriona38@hotmail.com, a.oriona@udc.es (Á. López-Oriona), jose.vilarf@udc.es (J.A. Vilar).

https://doi.org/10.1016/j.ins.2022.10.048
0020-0255/

GARCH coefficients [5], B-splines representations [11] and estimated conditional moments [12]. Alonso et al. [13] introduced cophenetic distances based on linear dependency. Cerqueti et al. [14] proposed a fuzzy clustering approach based on an optimal combination of conditional and unconditional moments. The method was applied to perform clustering of financial time series obtaining interesting results.

A large number of works in time series data mining have also considered spectral dissimilarity measures due to their high ability to discriminate between different dependence models. Kakizawa et al. [15] proposed a classification method based on a divergence measure between spectral matrices characterizing each MTS in a given dataset. Caiado et al. [16] developed hierarchical and non–hierarchical clustering of UTS on the basis of comparing normalized periodograms. Maharaj and D'Urso [17] designed a fuzzy clustering technique for UTS using cepstral coefficients, and an extension incorporating weights for each coefficient was proposed in [18] for clustering financial time series. A consistent estimate of the quantile cross-spectral density was considered by López-Oriona and Vilar [10] to perform crisp clustering of MTS, extending later this strategy to a fuzzy framework [19–21].

Spectral analysis has also played an important role in the context of hypothesis tests for time series. In particular, the problem of testing the equality of spectral densities has found a substantial interest in the literature. Swanepoel and Van Wyk [22] proposed different test statistics to compare the spectral densities of two independent stationary processes, obtaining the corresponding critical values by means of a bootstrap procedure. Timmer et al. [23] introduced a bootstrap test for checking for differences between spectral peak frequencies. The procedure consists of drawing new realizations of the periodograms from two estimated spectra to reestimate the spectra and compute the distribution of the peak frequency difference. Maharaj [24] devised an approach to compare the evolutionary spectra of two non-stationary time series. Randomization tests are carried out on groups of spectral estimates for both related and independent series. Fokianos and Savvides [25] compared spectral densities of several independent stationary processes by means of a novel semiparametric log-linear model linking all the spectral densities under study. Dette and Paparoditis [26] proposed a bootstrap procedure to approximate the null distribution of non-parametric test statistics about the spectral density matrix of a MTS. The asymptotic validity of the proposed approach is established under a set of general assumptions. Preuß et al. [27] proposed a test for comparing spectral densities of stationary time series with unequal sample sizes. The procedure generalizes a class of tests [28] based on estimating the L^2-distance between the spectral density and its best approximation under the null hypothesis. Jentsch and Pauly [29] constructed a non-parametric test through an L^2-type statistic and calculated the critical values with the help of randomization methods. More recently, a new approach for comparing the spectral densities of two independent periodically correlated time series has been provided by Mahmoudi et al. [30].

The aim of the present work is to introduce procedures to test that the quantile cross-spectral densities (QCD) of two independent MTS are equal. Specifically, let $\boldsymbol{X}_t^{(1)}$ and $\boldsymbol{X}_t^{(2)}$ be two independent, d-variate, real-valued strictly stationary stochastic processes. Fixed a frequency $\omega \in [-\pi, \pi]$ and a couple of probability levels, $\tau, \tau' \in [0,1]$, denote by $\mathfrak{f}^{(i)}(\omega, \tau, \tau')$, for $i = 1, 2$, the corresponding QCD matrices. The hypotheses we consider can be stated as

$$H_0 : \mathfrak{f}_{\boldsymbol{X}_t^{(1)}} = \mathfrak{f}_{\boldsymbol{X}_t^{(2)}} \quad \text{against} \quad H_1 : \mathfrak{f}_{\boldsymbol{X}_t^{(1)}} \neq \mathfrak{f}_{\boldsymbol{X}_t^{(2)}}, \tag{1}$$

where $\mathfrak{f}_{\boldsymbol{X}_t^{(1)}}$ and $\mathfrak{f}_{\boldsymbol{X}_t^{(2)}}$ are the sets of QCD matrices defined by

$$\mathfrak{f}_{\boldsymbol{X}_t^{(i)}} = \left\{ \mathfrak{f}^{(i)}(\omega, \tau, \tau'), \omega \in [-\pi, \pi], \tau, \tau' \in [0,1] \right\}, \text{ for } i = 1, 2. \tag{2}$$

In order to perform the hypothesis test in (1), we consider a distance measure between stationary stochastic processes, so-called d_{QCD}, which has already been used in several MTS data mining tasks [10,19–21]. The distance d_{QCD} works as follows. First, finite subsets of $\mathfrak{f}_{\boldsymbol{X}_t^{(1)}}$ and $\mathfrak{f}_{\boldsymbol{X}_t^{(2)}}$ in (2) are obtained by using a prefixed set of frequencies and probability levels. Then, d_{QCD} measures the Euclidean distance between the complex-valued vectors constructed by concatenating the terms of these subsets. Since the null hypothesis is true iff d_{QCD} is zero for every possible set of frequencies and probability levels, a test statistic based on this metric is a suitable tool to carry out the test in (1).

One of the main advantages of our approach is the high capability of d_{QCD} to describe any kind of dependence structure behind a given MTS. Compared to the spectral density, the quantile cross-spectral density basically replaces covariances and means by copulas and quantiles, thus being capable of providing a much richer picture of the underlying serial and cross-dependency structure [31]. This way, d_{QCD} has potential to detect differences between two stochastic processes which would stay hidden by using other distances considered in the literature [19]. The tests based on QCD are consistent, in the sense that, for a prefixed level, their power tends to one when the series have been generated from different processes. Note that this is not the case with traditional test statistics. For instance, two MTS can have the same cross-correlations (or classical cross-spectral densities) but different dependence structures.

Several methods for testing the hypotheses in (1) are introduced in this work. The first one is based on the asymptotic distribution of d_{QCD}. Applying results on the distribution of quadratic forms of normal random vectors, we establish that d_{QCD} can be asymptotically approximated by using a linear combination of central chi-square variables. However, obtaining the distribution limit is computationally intensive, which makes the corresponding test quite slow. The second method falls within the class of frequency domain bootstrap tests. We show that the hypotheses in (1) expressed in terms of d_{QCD} are a particular case of the general class of hypotheses defined by Dette and Paparoditis [26]. Therefore, we adapt the general bootstrap procedure proposed in [26] and verify that the set of assumptions required to ensure its asymptotic validity are

met. The crucial step of the procedure relies on the fact that QCD is the traditional spectral density for a specific bivariate process, which enables us to generate pseudo-periodogram matrices under the null in order to approximate the distribution of the test statistic. Lastly, we also consider two additional bootstrap approaches specifically designed to deal with dependent data, namely the moving blocks bootstrap (MBB) [32,33] and the stationary bootstrap (SB) [34]. In both cases, the key principle is to generate pseudo-series with the aim of mimicking the distribution under the null of a proper estimate of d_{QCD} without assuming specific parametric models for the generating processes.

The four approaches are compared in terms of size and power by means of a broad simulation study. Several types of generating processes are considered under the null and alternative hypotheses. Finally, the tests are applied to answer the question about whether or not the dotcom bubble burst of 2000s changed the global behaviour of financial markets.

The rest of the article is organized as follows. The distance d_{QCD} between stochastic processes is defined in Section 2. The four techniques to carry out the test in (1) are presented in Sections 3 and 4. While the asymptotic test is developed in Section 3, the bootstrap approaches are described in Section 4. The results from the simulation study performed to compare the proposed tests are reported in Section 5. Section 6 contains the financial application and Section 7 concludes. The appendices show how the asymptotic test proposed in Section 3 meets the assumptions required in [26].

2. A distance measure between stochastic processes

Let $\{\boldsymbol{X}_t, t \in \mathbb{Z}\} = \{(X_{t,1}, \ldots, X_{t,d}), t \in \mathbb{Z}\}$ be a d-variate real-valued strictly stationary stochastic process. Denote by F_j the marginal distribution function of $X_{t,j}, j = 1, \ldots, d$, and by $q_j(\tau) = F_j^{-1}(\tau), \tau \in [0,1]$, the corresponding quantile function. Fixed $l \in \mathbb{Z}$ and an arbitrary pair of quantile levels $(\tau, \tau') \in [0,1]^2$, consider the cross-covariance of the indicator functions $I\left\{X_{t,j_1} \leqslant q_{j_1}(\tau)\right\}$ and $I\left\{X_{t+l,j_2} \leqslant q_{j_2}(\tau')\right\}$ given by

$$\gamma_{j_1 j_2}(l, \tau, \tau') = \mathrm{Cov}\left(I\left\{X_{t,j_1} \leqslant q_{j_1}(\tau)\right\}, I\left\{X_{t+l,j_2} \leqslant q_{j_2}(\tau')\right\}\right),$$

for $1 \leqslant j_1, j_2 \leqslant d$. Taking $j_1 = j_2 = j$, the function $\gamma_{jj}(l, \tau, \tau')$, with $(\tau, \tau') \in [0,1]^2$, so-called quantile autocovariance function (QAF) of lag l, generalizes the traditional autocovariance function.

Under suitable summability conditions (mixing conditions), the Fourier transform of the cross-covariances is well-defined and the *quantile cross-spectral density* (QCD) is given by

$$\mathfrak{f}_{j_1 j_2}(\omega, \tau, \tau') = (1/2\pi) \sum_{l=-\infty}^{\infty} \gamma_{j_1 j_2}(l, \tau, \tau') e^{-il\omega}, \tag{3}$$

for $1 \leqslant j_1, j_2 \leqslant d, \omega \in \mathbb{R}$ and $\tau, \tau' \in [0,1]$. Note that $\mathfrak{f}_{j_1 j_2}(\omega, \tau, \tau')$ is complex-valued so that it can be represented in terms of its real and imaginary parts, which will be denoted by $\Re\left(\mathfrak{f}_{j_1 j_2}(\omega, \tau, \tau')\right)$ and $\Im\left(\mathfrak{f}_{j_1 j_2}(\omega, \tau, \tau')\right)$, respectively.

For fixed quantile levels (τ, τ'), QCD is the cross-spectral density of the bivariate process $\left(I\left\{X_{t,j_1} \leqslant q_{j_1}(\tau)\right\}, I\left\{X_{t,j_2} \leqslant q_{j_2}(\tau')\right\}\right)$. Therefore, QCD measures dependence between two components of the multivariate process over different ranges of their joint distribution and across frequencies. In order to obtain a complete representation of the process, we can evaluate QCD for every couple of components on a range of frequencies Ω and of quantile levels $\mathscr{T}$, i.e., consider the set of matrices

$$\mathfrak{f}_{\boldsymbol{X}_t}(\Omega, \mathscr{T}) = \{\mathfrak{f}(\omega, \tau, \tau'),\ \omega \in \Omega,\ \tau, \tau' \in \mathscr{T}\},$$

where $\mathfrak{f}(\omega, \tau, \tau')$ denotes the $d \times d$ matrix in $\mathbb{C}$ given by

$$\mathfrak{f}(\omega, \tau, \tau') = \left(\mathfrak{f}_{j_1 j_2}(\omega, \tau, \tau')\right)_{1 \leqslant j_1 j_2 \leqslant d}.$$

Representing $\boldsymbol{X}_t$ through $\mathfrak{f}_{\boldsymbol{X}_t}$, we have a valuable picture of both serial dependence and cross-sectional dependence of the process. Comprehensive discussions about the nice properties of the quantile cross-spectral density are given in Baruník and Kley [31] and López-Oriona et al. [19].

Based on these arguments, a dissimilarity measure between two multivariate processes, $\boldsymbol{X}_t^{(1)}$ and $\boldsymbol{X}_t^{(2)}$, could be established by comparing their respective representations in terms of the QCD matrices, $\mathfrak{f}_{\boldsymbol{X}_t^{(1)}}$ and $\mathfrak{f}_{\boldsymbol{X}_t^{(2)}}$, evaluated on a common range of frequencies and quantile levels. Specifically, for a given set of K different frequencies, $\Omega = \{\omega_1, \ldots, \omega_K\}$, and r quantile levels, $\mathscr{T} = \{\tau_1, \ldots, \tau_r\}$, each stochastic process $\boldsymbol{X}_t^{(u)}, u = 1, 2$, is characterized by means of a set of r^2 vectors $\{\boldsymbol{\Psi}^{(u)}_{\tau_i, \tau_{i'}}, 1 \leqslant i, i' \leqslant r\}$ given by

$$\boldsymbol{\Psi}^{(u)}_{\tau_i, \tau_{i'}} = \left(\boldsymbol{\Psi}^{(u)}_{1, \tau_i, \tau_{i'}}, \ldots, \boldsymbol{\Psi}^{(u)}_{K, \tau_i, \tau_{i'}}\right), \tag{4}$$

where each $\boldsymbol{\Psi}^{(u)}_{k, \tau_i, \tau_{i'}}, k = 1, \ldots, K$, denotes the vector of length d^2 formed by rearranging by rows the elements of the matrix $\mathfrak{f}(\omega_k, \tau_i, \tau_{i'})$.

Once the set of r^2 vectors $\boldsymbol{\Psi}^{(u)}_{\tau_i,\tau_{i'}}$ is obtained, they are all concatenated in a vector $\boldsymbol{\Psi}^{(u)}$ in the same way as vectors $\boldsymbol{\Psi}^{(u)}_{k,\tau_i,\tau_{i'}}$ constitute $\boldsymbol{\Psi}^{(u)}_{\tau_i,\tau_{i'}}$ in (4). Then, we define the dissimilarity between $\boldsymbol{X}_t^{(1)}$ and $\boldsymbol{X}_t^{(2)}$ by means of

$$d_{QCD}\left(\boldsymbol{X}_t^{(1)},\boldsymbol{X}_t^{(2)}\right) = \|\boldsymbol{\Psi}^{(1)} - \boldsymbol{\Psi}^{(2)}\|, \tag{5}$$

where $\|\boldsymbol{v}\| = \left(\sum_{k=1}^{n} |v_k|^2\right)^{1/2}$, with $\boldsymbol{v} = (v_1,\ldots,v_n)$ being an arbitrary complex vector in $\mathbb{C}^n$ and $|\cdot|$ stands for the modulus of a complex number. Note that d_{QCD} in (5) can also be expressed as

$$d_{QCD}\left(\boldsymbol{X}_t^{(1)},\boldsymbol{X}_t^{(2)}\right) = \left[\|\Re_v(\boldsymbol{\Psi}^{(1)}) - \Re_v(\boldsymbol{\Psi}^{(2)})\|^2 + \|\Im_v(\boldsymbol{\Psi}^{(1)}) - \Im_v(\boldsymbol{\Psi}^{(2)})\|^2\right]^{1/2},$$

where $\Re_v$ and $\Im_v$ denote the element-wise real and imaginary part operators, respectively.

Since, in practice, we only have finite-length realizations of the processes $\boldsymbol{X}_t^{(1)}$ and $\boldsymbol{X}_t^{(2)}$, the value of d_{QCD} is unknown and must be properly estimated.

Let $\{\boldsymbol{X}_1,\ldots,\boldsymbol{X}_T\}$ be a realization from the process $(\boldsymbol{X}_t)_{t\in\mathbb{Z}}$ so that $\boldsymbol{X}_t = (X_{t,1},\ldots,X_{t,d}), t = 1,\ldots,T$. For arbitrary $j_1,j_2 \in \{1,\ldots,d\}$ and $(\tau,\tau') \in [0,1]^2$, Baruník and Kley [31] propose to estimate $\mathfrak{f}_{j_1 j_2}(\omega,\tau,\tau')$ using a smoother of the cross-periodograms based on the indicator functions $I\left\{\widehat{F}_{Tj}(X_{tj})\right\}$, where $\widehat{F}_{Tj}(x) = T^{-1}\sum_{t=1}^{T} I\{X_{tj} \leqslant x\}$ denotes the empirical distribution function of X_{tj}. This approach extends to the multivariate case the estimator proposed by Kley et al. [35] in the univariate setting. More specifically, the called *rank-based copula cross periodogram* (CCR-periodogram) is defined by

$$I^{j_1 j_2}_{T,R}(\omega,\tau,\tau') = \frac{1}{2\pi T} d^{j_1}_{T,R}(\omega,\tau) d^{j_2}_{T,R}(-\omega,\tau'),$$

where

$$d^{j}_{T,R}(\omega,\tau) = \sum_{t=1}^{T} I\left\{\widehat{F}_{Tj}(X_{tj}) \leqslant \tau\right\} e^{-i\omega t}.$$

The asymptotic properties of the CCR-periodogram are established in Proposition S4.1 of [31]. Likewise the standard cross-periodogram, the CCR-periodogram is not a consistent estimate of $\mathfrak{f}_{j_1 j_2}(\omega,\tau,\tau')$. To achieve consistency, the CCR-periodogram ordinates (evaluated on the Fourier frequencies) are convolved with weighting functions $W_T(\cdot)$. The *smoothed CCR-periodogram* takes the form

$$\widehat{G}^{j_1 j_2}_{T,R}(\omega,\tau,\tau') = \frac{2\pi}{T}\sum_{s=1}^{T-1} W_T\left(\omega - \frac{2\pi s}{T}\right) I^{j_1 j_2}_{T,R}\left(\frac{2\pi s}{T},\tau,\tau'\right), \tag{6}$$

where

$$W_T(u) = \sum_{v=-\infty}^{\infty} \frac{1}{h_T} W\left(\frac{u+2\pi v}{h_T}\right),$$

with $h_T > 0$ a sequence of bandwidths such that $h_T \to 0$ and $Th_T \to \infty$ as $T \to \infty$, and W is a real-valued, even weight function with support $[-\pi,\pi]$. Consistency and asymptotic performance of the smoothed CCR-periodogram $\widehat{G}^{j_1 j_2}_{T,R}(\omega,\tau,\tau')$ are established in Theorem S4.1 of [31].

By considering the smoothed CCR-periodogram for every component of the vectors $\boldsymbol{\Psi}^{(1)}$ and $\boldsymbol{\Psi}^{(2)}$, we obtain their estimated counterparts $\hat{\boldsymbol{\Psi}}^{(1)}$ and $\hat{\boldsymbol{\Psi}}^{(2)}$, which allow to construct a consistent estimate of d_{QCD} by defining

$$\hat{d}_{QCD}\left(\boldsymbol{X}_t^{(1)},\boldsymbol{X}_t^{(2)}\right) = \|\hat{\boldsymbol{\Psi}}^{(1)} - \hat{\boldsymbol{\Psi}}^{(2)}\|. \tag{7}$$

The statistic $\hat{d}_{QCD}\left(\boldsymbol{X}_t^{(1)},\boldsymbol{X}_t^{(2)}\right)$ has been successfully applied to perform clustering of MTS in crisp [10] and fuzzy [19–21] frameworks.

In upcoming sections, several procedures to address the problem of testing (1) are constructed. All of them are based on the distance d_{QCD} defined in (5).

3. Testing for equality of quantile cross-spectral densities on the basis of the asymptotic distribution of $\widehat{d}_{QCD}$

The first testing procedure is based on the asymptotic distribution of the estimate $\widehat{d}_{QCD}$. Applying an important result about the distribution of a general quadratic form of a normal random vector, the limiting distribution of $\widehat{d}_{QCD}$ is stated and used for testing the hypotheses in (1).

3.1. Distribution of quadratic forms of a normal random vector

In this section, we follow some arguments given in [36]. Let $\boldsymbol{Y} = (Y_1, \ldots, Y_p)^\intercal$ be a p-variate random vector having a normal distribution with expectation vector $\boldsymbol{\mu}$ and covariance matrix Σ. Given the matrix $L \in Sym_p(\mathbb{R})$, consider the quadratic form

$$Q(\boldsymbol{Y}) = \boldsymbol{Y}^\intercal L \boldsymbol{Y} = \sum_{i=1}^{p}\sum_{j=1}^{p} l_{ij} Y_i Y_j. \tag{8}$$

Assuming that Σ is invertible, the vector $\boldsymbol{Z} = \Sigma^{-1/2}(\boldsymbol{Y} - \boldsymbol{\mu})$ follows a standard multivariate normal distribution, and we can write

$$Q(\boldsymbol{Y}) = \left(\boldsymbol{Z} + \Sigma^{-1/2}\boldsymbol{\mu}\right)^\intercal \Sigma^{1/2} L \Sigma^{1/2} \left(\boldsymbol{Z} + \Sigma^{-1/2}\boldsymbol{\mu}\right).$$

Applying the spectral theorem for symmetric matrices to the symmetric matrix $\Sigma^{1/2} L \Sigma^{1/2}$, we have $\Sigma^{1/2} L \Sigma^{1/2} = P^\intercal \Lambda P$, where P is an orthogonal matrix (so that $PP^\intercal = P^\intercal P = I$), and $\Lambda = \mathrm{diag}(\lambda_1, \ldots, \lambda_p)$ with positive diagonal entries consisting of the eigenvalues of the matrix $\Sigma^{1/2} L \Sigma^{1/2}$. Define now $\boldsymbol{R} = P\boldsymbol{Z}$ so that $\boldsymbol{R} = (R_1, \ldots, R_p)^\intercal$ is multivariate normal with expectation zero and identity covariance matrix. Taking into account the previous considerations, we can express now the quadratic form as

$$Q(\boldsymbol{Y}) = \left(\boldsymbol{Z} + \Sigma^{-1/2}\boldsymbol{\mu}\right)^\intercal P^\intercal \Lambda P \left(\boldsymbol{Z} + \Sigma^{-1/2}\boldsymbol{\mu}\right) = \left(P\boldsymbol{Z} + P\Sigma^{-1/2}\boldsymbol{\mu}\right)^\intercal \Lambda \left(P\boldsymbol{Z} + P\Sigma^{-1/2}\boldsymbol{\mu}\right) = (\boldsymbol{R} + \boldsymbol{b})^\intercal \Lambda (\boldsymbol{R} + \boldsymbol{b}),$$

where $\boldsymbol{b} = P\Sigma^{-1/2}\boldsymbol{\mu}$. Hence

$$Q(\boldsymbol{Y}) = \boldsymbol{Y}^\intercal L \boldsymbol{Y} = \sum_{i=1}^{p} \lambda_i (R_i + b_i)^2.$$

Therefore, the quadratic form $Q(\boldsymbol{Y})$ has the distribution of a linear combination of independent, non-central, chi-square variables, with the coefficients of the combination given by the eigenvalues of $\Sigma^{1/2} L \Sigma^{1/2}$. The distribution function of a linear combination of independent chi-square variables has been extensively studied (see e.g., [37] for the central case and [38] for the non-central case). The R-package CompQuadForm [39] provides a framework for working numerically with these types of distributions.

3.2. Asymptotic distribution of $\widehat{d}_{QCD}$

Given two independent realizations of length T from the d-variate stochastic processes $\boldsymbol{X}_t^{(1)}$ and $\boldsymbol{X}_t^{(2)}$, consider the distance measure $\hat{d}_{QCD}\left(\boldsymbol{X}_t^{(1)}, \boldsymbol{X}_t^{(2)}\right) = \|\hat{\boldsymbol{\Psi}}^{(1)} - \hat{\boldsymbol{\Psi}}^{(2)}\|$ introduced in (7). For the sake of simplicity, the elements of the complex random vector of smoothed CCR-periodograms $\hat{\boldsymbol{\Psi}}^{(i)}, i = 1, 2$, are indexed by a unique index v ranging from 1 to $m = Kd^2r^2$, thus denoting $\hat{\boldsymbol{\Psi}}^{(i)} = \left(\hat{\Psi}_1^{(i)}, \ldots, \hat{\Psi}_m^{(i)}\right)^\intercal$. Note that each value of the index is really associated to a specific 5-tuple of indexes, $v = (v_1, v_2, v_3, v_4, v_5)$, whose components indicate: a pair of probability levels (τ_{v_1}, τ_{v_2}), with $1 \leqslant v_1, v_2 \leqslant r$, a pair of dimensions $\left(j_{v_3}, j_{v_4}\right)$, with $1 \leqslant v_3, v_4 \leqslant d$, and a single frequency ω_{v_5}, with $1 \leqslant v_5 \leqslant K$. Analogously, the corresponding vectors of quantile cross-spectral densities are denoted by $\boldsymbol{\Psi}^{(i)} = \left(\Psi_1^{(i)}, \ldots, \Psi_m^{(i)}\right)^\intercal, i = 1, 2$. From Theorem S4.1 in [31], we can state that the vector $\boldsymbol{E}^{(i)} = \sqrt{Th_T}\left(\hat{\boldsymbol{\Psi}}^{(i)} - \boldsymbol{\Psi}^{(i)}\right), i = 1, 2$, asymptotically follows a circularly-symmetric Gaussian distribution characterized by the covariance matrix $\Gamma^{(i)}$, whose (v, s)-element, for $v, s = 1, \ldots, m$, is given by

$$\Gamma_{v,s}^{(i)} = \mathrm{Cov}\left(E_v^{(i)}, E_s^{(i)}\right) = A(B_{v,s} + C_{v,s}) + \zeta, \tag{9}$$

where $\zeta \approx 0$ is a negligible term provided that the bandwidth h_T is chosen accordingly, and

$$\begin{aligned} A &= 2\pi\left(\textstyle\int_{-\pi}^{\pi} W^2(\alpha) d\alpha\right), \\ B_{v,s} &= \tilde{\mathfrak{f}}_{j_{v_3} j_{s_3}}^{(i)}(\omega_{v_5}, \tau_{v_1}, \tau_{s_1})\, \tilde{\mathfrak{f}}_{j_{v_4} j_{s_4}}^{(i)}(-\omega_{v_5}, \tau_{v_2}, \tau_{s_2})\, \eta(\omega_{v_5} - \omega_{s_5}), \\ C_{v,s} &= \tilde{\mathfrak{f}}_{j_{v_3} j_{s_4}}^{(i)}(\omega_{v_5}, \tau_{v_1}, \tau_{s_2})\, \tilde{\mathfrak{f}}_{j_{v_4} j_{s_3}}^{(i)}(-\omega_{v_5}, \tau_{v_2}, \tau_{s_1})\, \eta(\omega_{v_5} + \omega_{s_5}), \end{aligned} \tag{10}$$

being $\eta(x) = I\{x = 0(\mathrm{mod} 2\pi)\}$ the 2π-periodic extension of Kroneckers's delta function. An estimator $\widehat{\Gamma}^{(i)}$ of $\Gamma^{(i)}$ can be obtained by replacing in (9) the unknown terms $B_{v,s}$ and $C_{v,s}$ by the estimates $\widehat{B}_{v,s}$ and $\widehat{C}_{v,s}$ based on the corresponding smoothed CCR-periodograms given in (6).

Now, for $i = 1, 2$, denote by

$$\hat{\boldsymbol{\Theta}}^{(i)} = \left(\Re\left(\hat{\Psi}_1^{(i)}\right), \ldots, \Re\left(\hat{\Psi}_m^{(i)}\right), \Im\left(\hat{\Psi}_1^{(i)}\right), \ldots, \Im\left(\hat{\Psi}_m^{(i)}\right)\right)^{\intercal}$$

the estimate of the vector obtained by concatenating the real and imaginary parts in $\Psi^{(i)}$, i.e., $\boldsymbol{\Theta}^{(i)} = \left(\Re\left(\Psi_1^{(i)}\right), \ldots, \Re\left(\Psi_m^{(i)}\right), \Im\left(\Psi_1^{(i)}\right), \ldots, \Im\left(\Psi_m^{(i)}\right)\right)^{\intercal}$. From the circularly symmetrical character of the vector $\boldsymbol{E}^{(i)}$ and its asymptotic behavior follows that the real random vector $\sqrt{Th_T}\left(\hat{\boldsymbol{\Theta}}^{(i)} - \boldsymbol{\Theta}^{(i)}\right)$ is asymptotically normally distributed with zero mean and covariance matrix $\widehat{\Sigma}^{(i)}$ given by

$$\widehat{\Sigma}^{(i)} = \frac{1}{2}\begin{bmatrix} \Re\left(\widehat{\Gamma}^{(i)}\right) & -\Im\left(\widehat{\Gamma}^{(i)}\right) \\ \Im\left(\widehat{\Gamma}^{(i)}\right) & \Re\left(\widehat{\Gamma}^{(i)}\right) \end{bmatrix}.$$

Furthermore, as we deal with independent realizations, it also holds that the vector $\sqrt{Th_T}\left(\left(\hat{\boldsymbol{\Theta}}^{(1)} - \boldsymbol{\Theta}^{(1)}\right) - \left(\hat{\boldsymbol{\Theta}}^{(2)} - \boldsymbol{\Theta}^{(2)}\right)\right)$ is asymptotically normal distributed with zero mean and covariance matrix $\widehat{\Sigma}^{(1)} + \widehat{\Sigma}^{(2)}$.

Now, since the square of the estimated QCD-distance between $\boldsymbol{X}_t^{(1)}$ and $\boldsymbol{X}_t^{(2)}$ can be written as

$$\hat{d}^2_{QCD}\left(\boldsymbol{X}_t^{(1)}, \boldsymbol{X}_t^{(2)}\right) = \left(\hat{\boldsymbol{\Theta}}^{(1)} - \hat{\boldsymbol{\Theta}}^{(2)}\right)^{\intercal}\left(\hat{\boldsymbol{\Theta}}^{(1)} - \hat{\boldsymbol{\Theta}}^{(2)}\right), \tag{11}$$

we have

$$\begin{aligned} &\sqrt{Th_T}\left[\hat{\boldsymbol{\Theta}}^{(1)} - \hat{\boldsymbol{\Theta}}^{(2)} - \left(\boldsymbol{\Theta}^{(1)} - \boldsymbol{\Theta}^{(2)}\right)\right]^{\intercal}\left[\hat{\boldsymbol{\Theta}}^{(1)} - \hat{\boldsymbol{\Theta}}^{(2)} - \left(\boldsymbol{\Theta}^{(1)} - \boldsymbol{\Theta}^{(2)}\right)\right]\sqrt{Th_T} = \\ &Th_T\left[\hat{d}^2_{QCD}\left(\boldsymbol{X}_t^{(1)}, \boldsymbol{X}_t^{(2)}\right) - 2\left(\boldsymbol{\Theta}^{(1)} - \boldsymbol{\Theta}^{(2)}\right)^{\intercal}\left(\hat{\boldsymbol{\Theta}}^{(1)} - \hat{\boldsymbol{\Theta}}^{(2)}\right) + \|\boldsymbol{\Theta}^{(1)} - \boldsymbol{\Theta}^{(2)}\|^2\right]. \end{aligned} \tag{12}$$

The first term of the equality in (12) corresponds to a quadratic form of an asymptotically normal random vector in the terms of (8). In fact, it is enough to consider $\boldsymbol{Y} = \sqrt{Th_T}\left[\hat{\boldsymbol{\Theta}}^{(1)} - \hat{\boldsymbol{\Theta}}^{(2)} - \left(\boldsymbol{\Theta}^{(1)} - \boldsymbol{\Theta}^{(2)}\right)\right]$, $\boldsymbol{\mu} = \boldsymbol{0}$, $\Sigma = \hat{\Sigma}^{(1)} + \hat{\Sigma}^{(2)}$, and L the identity matrix. Hence, the same arguments employed in Section 3.1 allow us to conclude that

$$\begin{aligned} &Th_T\left[\hat{d}^2_{QCD}\left(\boldsymbol{X}_t^{(1)}, \boldsymbol{X}_t^{(2)}\right) - 2\left(\boldsymbol{\Theta}^{(1)} - \boldsymbol{\Theta}^{(2)}\right)^{\intercal}\left(\hat{\boldsymbol{\Theta}}^{(1)} - \hat{\boldsymbol{\Theta}}^{(2)}\right) + \|\boldsymbol{\Theta}^{(1)} - \boldsymbol{\Theta}^{(2)}\|^2\right] \\ &\qquad \xrightarrow{d} \sum_{i=1}^{2m} \lambda_i R_i^2, \text{ as } T \to \infty, \end{aligned} \tag{13}$$

where $\lambda_1, \ldots, \lambda_{2m}$ are the eigenvalues of $\Sigma = \widehat{\Sigma}^{(1)} + \widehat{\Sigma}^{(2)}$ and $R_1, \ldots, R_{2m}$ are mutually independent standard normal variables. Therefore, the limit distribution in (13) is a linear combination of central chi-square variables with coefficients determined by the matrix $\widehat{\Sigma}^{(1)} + \widehat{\Sigma}^{(2)}$. We denote this distribution by $D^2_{QCD}\left(\widehat{\Gamma}^{(1)}, \widehat{\Gamma}^{(2)}\right)$.

3.3. The hypothesis test

The asymptotic distribution derived in (13) can be used to test for equality of the quantile cross-spectral densities of the stochastic processes $\boldsymbol{X}_t^{(1)}$ and $\boldsymbol{X}_t^{(2)}$, as stated in (1). The hypotheses in (1) are replaced by

$$H_0 : d_{QCD}\left(\boldsymbol{X}_t^{(1)}, \boldsymbol{X}_t^{(2)}\right) = 0 \quad \text{against} \quad H_1 : d_{QCD}\left(\boldsymbol{X}_t^{(1)}, \boldsymbol{X}_t^{(2)}\right) > 0, \tag{14}$$

or, equivalently, by

$$H_0 : d^2_{QCD}\left(\boldsymbol{X}_t^{(1)}, \boldsymbol{X}_t^{(2)}\right) = 0 \quad \text{against} \quad H_1 : d^2_{QCD}\left(\boldsymbol{X}_t^{(1)}, \boldsymbol{X}_t^{(2)}\right) > 0. \tag{15}$$

Note that the hypothesis tests in (14) and (15) are not consistent, since the discretisation on the quantile levels does not guarantee that $d_{QCD}\left(\boldsymbol{X}_t^{(1)}, \boldsymbol{X}_t^{(2)}\right) > 0$ if $\boldsymbol{X}_t^{(1)}$ and $\boldsymbol{X}_t^{(2)}$ are different stochastic processes. However, in practice, a small set of probability levels has proven to be enough to capture most types of discrepancies [10,19].

Under the null hypothesis, the two MTS come from the same generating process so that $\boldsymbol{\Theta}^{(1)} = \boldsymbol{\Theta}^{(2)}$. Then, from (13) follows that the asymptotic distribution of the test statistic under the null becomes

$$Th_T\,\hat{d}^2_{QCD}\left(\boldsymbol{X}_t^{(1)}, \boldsymbol{X}_t^{(2)}\right) \sim \sum_{i=1}^{2m} \lambda_i R_i^2. \tag{16}$$

The null hypothesis must be rejected for large values of the test statistic. Hence, for a given significance level $\alpha \in (0, 1)$, the decision rule consists of rejecting H_0 if

$$Th_T\,\hat{d}^2_{QCD}\left(\boldsymbol{X}_t^{(1)},\boldsymbol{X}_t^{(2)}\right) \;>\; D^2_{QCD}\left(\widehat{\Gamma}^{(1)},\widehat{\Gamma}^{(2)}\right)_{1-\alpha},$$

where $D^2_{QCD}\left(\widehat{\Gamma}^{(1)},\widehat{\Gamma}^{(2)}\right)_{1-\alpha}$ denotes the $(1-\alpha)$-quantile in the distribution $D^2_{QCD}\left(\widehat{\Gamma}^{(1)},\widehat{\Gamma}^{(2)}\right)$.

4. Testing for equality of quantile cross-spectral densities by means of bootstrap procedures

Bootstrap methods provide an alternative way of approximating the null distribution of the test statistic $\widehat{d}_{QCD}$. In this section, three nonparametric resampling procedures based on bootstrapping $\widehat{d}_{QCD}$ are introduced. The first test is a frequency domain bootstrap approach whose asymptotic validity follows from the bootstrap central limit theorem established in [26]. The remaining two approaches consider well known bootstrap methods for dependent data. The key principle is to draw pseudo-series capturing the dependence structure without assuming any parametric model.

4.1. A frequency domain bootstrap test

The first bootstrap test follows the general bootstrap methodology developed by Dette and Paparoditis [26]. Specifically, the following general class of hypotheses is considered in [26]:

$$H_0 : \int_{-\pi}^{\pi} \|\varphi(g(\omega),\omega)\|^2\, d\omega = 0 \text{ against } H_1 : \int_{-\pi}^{\pi} \|\varphi(g(\omega),\omega)\|^2\, d\omega \;>\; 0, \tag{17}$$

where $g(\omega)$ denotes the spectral density matrix of the underlying m-dimensional stationary process, and $\varphi : D\times[-\pi,\pi]\to\mathbb{C}^r$ is some suitable vector-valued function specifying the particular null hypothesis of interest. It is assumed that D is an open subset of $\mathbb{C}^{m\times m}$ containing the spectral density matrices. Then, a test statistic for the general hypotheses in (17) can be obtained by replacing $g(\omega)$ by a nonparametric estimator $\widehat{g}(\omega)$, i.e., by considering

$$S_T(\varphi) = \int_{-\pi}^{\pi} \|\varphi(\widehat{g}(\omega),\omega)\|^2\, d\omega. \tag{18}$$

Assuming some regularity conditions on the function φ (Assumption 2 in [26]), Dette and Paparoditis introduce a general bootstrap method to correctly approximate the null distribution of $S_T(\varphi)$ based on two principles: (i) the pseudo-periodogram matrices generated to construct the bootstrap replicates of the test statistic must satisfy the null hypothesis even if this hypothesis is not true, and (ii) the prior condition is met when the estimated spectral density matrices used to generate the pseudo-periodograms satisfy the set of requirements summarized in Condition 1 in [26]. To adjust this approach to our framework, our aim was to construct suitable estimates of the quantile cross-spectral density matrices satisfying the requirements in Condition 1, which ensures the asymptotic validity of the bootstrap procedure according with Theorem 1 in [26].

We proceed as follows. Let $\boldsymbol{X}_t^{(1)} = \left\{\left(X_{t,1}^{(1)},\ldots,X_{t,d}^{(1)}\right), t\in\mathbb{Z}\right\}$ and $\boldsymbol{X}_t^{(2)} = \left\{\left(X_{t,1}^{(2)},\ldots,X_{t,d}^{(2)}\right), t\in\mathbb{Z}\right\}$ be two d-dimensional strictly stationary stochastic processes. Given the set of quantile levels $\mathscr{T} = \{\tau_1,\ldots,\tau_r\}$, define the process

$$\boldsymbol{Z}_t = \left(\boldsymbol{Z}_t^{(1)},\boldsymbol{Z}_t^{(2)}\right), \tag{19}$$

where

$$\boldsymbol{Z}_t^{(i)} = \left(\widetilde{Z}_1^{(i)}(\tau_1),\ldots\widetilde{Z}_1^{(i)}(\tau_r),\widetilde{Z}_2^{(i)}(\tau_1),\ldots\widetilde{Z}_2^{(i)}(\tau_r),\widetilde{Z}_d^{(i)}(\tau_1),\ldots\widetilde{Z}_d^{(i)}(\tau_r)\right),$$

with components

$$\widetilde{Z}_k^{(i)}(\tau_j) = I\left\{X_{t,k}^{(i)} \leqslant q_k^{(i)}(\tau_j)\right\} - \tau_j,$$

for $i=1,2, k=1,\ldots,d$, and $j=1,\ldots,r$, with $q_k^{(i)}(\cdot)$ being the quantile function of the k-th variable in the i-th process.

Since $\boldsymbol{Z}_t^{(1)}$ and $\boldsymbol{Z}_t^{(2)}$ are independent processes, the spectral density matrix of $\boldsymbol{Z}_t$, let us say $g_z(\omega)$, can be written as

$$g_z(\omega) = \begin{pmatrix} g_z^{(1)}(\omega) & 0_{rd} \\ 0_{rd} & g_z^{(2)}(\omega)\end{pmatrix},$$

where 0_{rd} denotes the square zero matrix of order rd, and $g_z^{(i)}(\omega)$ denotes the spectral density matrix of $\boldsymbol{Z}_t^{(i)}, i=1,2$, given by

$$g_z^{(i)}(\omega) = \begin{pmatrix} \mathfrak{f}_{1,1}^{(i)}(\omega) & \cdots & \mathfrak{f}_{1,d}^{(i)}(\omega) \\ \vdots & \ddots & \vdots \\ \mathfrak{f}_{d,1}^{(i)}(\omega) & \cdots & \mathfrak{f}_{d,d}^{(i)}(\omega)\end{pmatrix}, \text{ with } \mathfrak{f}_{l,s}^{(i)}(\omega) = \left(\mathfrak{f}_{l,s}^{(i)}(\omega,\tau_u,\tau_v)\right)_{1\leqslant u,v\leqslant r}. \tag{20}$$

Now, denote by $vec(\cdot)$ the operator that vectorizes a matrix concatenating by rows its elements and consider the following specification for the function φ in (17):

$$\varphi(g_z(\omega),\omega) = vec\left(g_z^{(1)}(\omega)\right) - vec\left(g_z^{(2)}(\omega)\right). \tag{21}$$

We have

$$\|\varphi(g_z(\omega),\omega)\| = d_{QCD,\omega}\left(\boldsymbol{X}_t^{(1)},\boldsymbol{X}_t^{(2)}\right),$$

where the subscript ω added to d_{QCD} indicates that the distance is only computed for the frequency ω. Hence, the general hypotheses in (17) become

$$H_0 : \int_{-\pi}^{\pi} d^2_{QCD,\omega}\left(\boldsymbol{X}_t^{(1)},\boldsymbol{X}_t^{(2)}\right) d\omega = 0 \text{ vs } H_1 : \int_{-\pi}^{\pi} d^2_{QCD,\omega}\left(\boldsymbol{X}_t^{(1)},\boldsymbol{X}_t^{(2)}\right) d\omega > 0. \tag{22}$$

This way, the test for equality of the quantile cross-spectral densities is stated as a particular case of the general specification introduced in (17) and in terms of QCD-distances. Given realizations of length T from $\boldsymbol{X}_t^{(1)}$ and $\boldsymbol{X}_t^{(2)}$, we proceed as in (18) and obtain a test statistic, $S_T(\varphi)$, replacing $d^2_{QCD,\omega}$ by their estimates $\widehat{d}^2_{QCD,\omega}$. In practice, the finite set of Fourier frequencies is used, thus giving rise to the test statistic $\hat{d}^2_{QCD}\left(\boldsymbol{X}_t^{(1)},\boldsymbol{X}_t^{(2)}\right)$, or simply $\hat{d}_{QCD}\left(\boldsymbol{X}_t^{(1)},\boldsymbol{X}_t^{(2)}\right)$.

The bootstrap procedure to approximate the distribution of the test statistic $\hat{d}_{QCD}\left(\boldsymbol{X}_t^{(1)},\boldsymbol{X}_t^{(2)}\right)$ under the null hypothesis is sketched as follows.

Step 1. Given the set of Fourier frequencies $\{\omega_k = 2\pi k/T, 1 \leqslant k \leqslant (T-1)\}$, generate two sets of $(T-1)$ independent matrices

$$I^{(i)*}(\omega_k) = \widehat{G}_z(\omega_k)^{1/2} W_k^* \widehat{G}_z(\omega_k)^{1/2},\ i = 1,2,$$

where $\widehat{G}_z(\omega_k)$ is given by

$$\widehat{G}_z(\omega_k) = \frac{1}{2}\left(\widehat{G}_z^{(1)}(\omega_k) + \widehat{G}_z^{(2)}(\omega_k)\right), \tag{23}$$

with $\hat{G}_z^{(i)}$ being the matrix of smoothed CCR-periodograms based on the realization of $\boldsymbol{Z}_t^{(i)}$ (i.e., an estimate of the spectral density matrix $g_z^{(i)}$ in (20)) and

$$W_k^* \sim \begin{cases} W^C(1, I_{dr}) & 1 \leqslant k \leqslant T/2 \\ W^R(1, I_{dr}) & k \in \{T/2\} \\ W_{T-k}^* & T/2 \leqslant k \leqslant (T-1), \end{cases}$$

where W^C and W^R denote the complex and real Wishart distributions and I_{dr} stands for the identity matrix of order dr.

Step 2. Construct the bootstrap quantile cross-spectral density matrices estimates, $\widehat{G}_z^{(i)*}(\omega_k), i = 1,2, k = 1,\ldots,T$, by smoothing $I^{(i)*}(\omega_k)$ in the form

$$\widehat{G}_z^{(i)*}(\omega_k) = \frac{2\pi}{T}\sum_{s=1}^{T-1} W_T(\omega_k - \omega_s) I^{(i)*}(\omega_s).$$

Step 3. Based on $\widehat{G}_z^{(1)*}$ and $\widehat{G}_z^{(2)*}$, construct the bootstrap version of $\hat{d}_{QCD}$, $\hat{d}^*_{QCD}$.

Step 4. Repeat Steps 1–3 a large number B of times to obtain the bootstrap replicates $\widehat{d}^{(1)*}_{QCD},\ldots,\widehat{d}^{(B)*}_{QCD}$.

Step 5. Given a significance level α, compute the quantile of order $1-\alpha$, $q^*_{1-\alpha}$, based on the set $\left\{\widehat{d}^{(1)*}_{QCD},\ldots,\widehat{d}^{(B)*}_{QCD}\right\}$. Then, the decision rule consists of rejecting H_0 if $\hat{d}_{QCD}\left(\boldsymbol{X}_t^{(1)},\boldsymbol{X}_t^{(2)}\right) > q^*_{1-\alpha}$.

A few remarks about the bootstrap procedure are given below.

Remark 1. The approach to build the pseudo-periodogram matrices $I^{(i)*}(\omega_k)$ in Step 1 is based on the fact that the periodogram matrix $I(\omega_k)$ of a strictly stationary process can be approximated by

$$I(\omega_k) = g^{1/2}(\omega_k) U(\omega_k) \overline{g}^{1/2}(\omega_k),$$

where the matrices $U(\omega_k), 1 \leqslant k \leqslant (T-1)$, are asymptotically independent, complex Wishart distributed if $\omega_k \neq 0(\mathrm{mod}\pi)$ and real Wishart distributed if $\omega_k = 0(\mathrm{mod}\pi)$ (see Section 11.7 in [40]). The spectral density matrix $g(\omega_k)$ is replaced by a proper estimate (see Remark 2 below).

Remark 2. The average matrix $\hat{G}_z(\omega_k)$ is used to construct $I^{(i)*}(\omega_k), i = 1, 2, k = 1, \ldots, (T-1)$. This choice constitutes a crucial point in the bootstrap procedure by ensuring that the estimate used to generate the bootstrap replicates, $\widehat{g}(\omega)$ in (18), satisfies the null hypothesis of interest.

Remark 3. Since our hypothesis testing problem fits into the general specification (17), the asymptotic validity of the proposed bootstrap method follows from Theorem 1 in [26], once the requirements of this result are shown to hold. Broadly speaking, these requirements involve: the existence of the spectral matrices of the underlying processes (*Assumption 1*), specific properties of the general function φ in (17) (*Assumption 2*), a set of regularity hypotheses on the kernel function W and the bandwidth h_T (*Assumptions 3* and *4*, respectively), and lastly a set of requirements imposed on the estimate $\widehat{g}(\omega)$ (*Condition 1*). We show in the Appendix that the bootstrap procedure constructed throughout this section verifies all the required assumptions.

From now on, we will refer to the test presented in this section as FDB (*Frequency Domain Bootstrap*).

4.2. A test based on the moving blocks bootstrap

In this section, we introduce an alternative bootstrap test based on a modification of the classical moving blocks bootstrap (MBB) method [32,33]. MBB generates replicates of the time series by joining blocks of fixed length, which have been drawn randomly with replacement from among blocks of the original realizations. This approach allows to mimic the underlying dependence structure without assuming specific parametric models for the generating processes.

Given two realizations of the d-dimensional stochastic processes $\boldsymbol{X}_t^{(1)}$ and $\boldsymbol{X}_t^{(2)}$, denoted by $\overline{\boldsymbol{X}}_t^{(1)} = \left\{\boldsymbol{X}_1^{(1)}, \ldots, \boldsymbol{X}_T^{(1)}\right\}$ and $\overline{\boldsymbol{X}}_t^{(2)} = \left\{\boldsymbol{X}_1^{(2)}, \ldots, \boldsymbol{X}_T^{(2)}\right\}$, respectively, the procedure proceeds as follows.

Step 1.Fix a positive integer, b, representing the block size, and take k equal to the smallest integer greater than or equal to T/b.

Step 2. For each realization, define the block $\boldsymbol{B}_j^{(i)} = \left\{\boldsymbol{X}_j^{(i)}, \ldots, \boldsymbol{X}_{j+b-1}^{(i)}\right\}$, for $j = 1, \ldots, q$, with $q = T - b + 1$. Let $\overline{\boldsymbol{B}} = \left\{\boldsymbol{B}_j^{(1)}, \ldots, \boldsymbol{B}_q^{(1)}, \boldsymbol{B}_j^{(2)}, \ldots, \boldsymbol{B}_q^{(2)}\right\}$ be the set of all blocks, that is including those coming from $\overline{\boldsymbol{X}}_t^{(1)}$ and from $\overline{\boldsymbol{X}}_t^{(2)}$.

Step 3. Draw two sets of k blocks, $\xi^{(i)} = \left\{\xi_1^{(i)}, \ldots, \xi_k^{(i)}\right\}, i = 1, 2$, with equiprobable distribution from $\overline{\boldsymbol{B}}$. Note that each $\xi_j^{(i)}, j = 1, \ldots, k, i = 1, 2$, is a b-dimensional MTS, let us say $\left(\xi_{1j}^{(i)}, \xi_{2j}^{(i)}, \ldots, \xi_{bj}^{(i)}\right)$.

Step 4. For each $i = 1, 2$, construct the pseudo-series $\overline{\boldsymbol{X}}_t^{(i)*}$ by taking the first T elements of:

$$\xi^{(i)} = \left(\xi_{11}^{(i)}, \xi_{21}^{(i)}, \ldots, \xi_{b1}^{(i)}, \xi_{12}^{(i)}, \xi_{22}^{(i)}, \ldots, \xi_{b2}^{(i)}, \ldots, \xi_{1k}^{(i)}, \xi_{2k}^{(i)}, \ldots, \xi_{bk}^{(i)}\right).$$

Then, obtain the bootstrap version $\widehat{d}_{QCD}^*$ of $\widehat{d}_{QCD}$ based on the pseudo-series $\overline{\boldsymbol{X}}_t^{(1)*}$ and $\overline{\boldsymbol{X}}_t^{(2)*}$.

Step 5. Repeat Steps 3 and 4 a large number B of times to obtain the bootstrap replicates $\widehat{d}_{QCD}^{(1)*}, \ldots, \widehat{d}_{QCD}^{(B)*}$.

Step 6. Given a significance level α, compute the quantile of order $1-\alpha$, $q_{1-\alpha}^*$, based on the set $\left\{\widehat{d}_{QCD}^{(1)*}, \ldots, \widehat{d}_{QCD}^{(B)*}\right\}$. Then, the decision rule consists of rejecting H_0 if $\hat{d}_{QCD}\left(\boldsymbol{X}_t^{(1)}, \boldsymbol{X}_t^{(2)}\right) > q_{1-\alpha}^*$.

Note that, by considering the whole set of blocks $\overline{\boldsymbol{B}}$ in Step 2, both pseudo-time series $\overline{\boldsymbol{X}}_t^{(1)*}$ and $\overline{\boldsymbol{X}}_t^{(2)*}$ contain information about the original series $\overline{\boldsymbol{X}}_t^{(1)}$ and $\overline{\boldsymbol{X}}_t^{(2)}$ in equal measure. This way, the bootstrap procedure is able to approximate correctly the distribution of the test statistic $\widehat{d}_{QCD}$ under the null hypothesis even if this hypothesis is not true.

From now on, we will refer to the test presented in this section as MBB.

4.3. A test based on the stationary bootstrap

The third bootstrap mechanism to approximate the distribution of $\widehat{d}_{QCD}$ adapts the classical stationary bootstrap (SB) [34]. This resampling method is aimed at overcoming the lack of stationarity of the MBB procedure. Note that d_{QCD} is well-defined only for stationary processes, so it is desirable that a bootstrap technique based on this metric generates stationary pseudo-series.

For two realizations $\overline{\boldsymbol{X}}_t^{(1)} = \left\{\boldsymbol{X}_1^{(1)}, \ldots, \boldsymbol{X}_T^{(1)}\right\}$ and $\overline{\boldsymbol{X}}_t^{(2)} = \left\{\boldsymbol{X}_1^{(2)}, \ldots, \boldsymbol{X}_T^{(2)}\right\}$ from the d-dimensional stochastic processes $\boldsymbol{X}_t^{(1)}$ and $\boldsymbol{X}_t^{(2)}$, respectively, the SB method proceeds as follows.

Step 1. Fix a positive real number $p \in [0, 1]$.

Step 2. Draw randomly two observations from the set $\widetilde{\boldsymbol{X}}_t = \left\{\overline{\boldsymbol{X}}_t^{(1)}, \overline{\boldsymbol{X}}_t^{(2)}\right\}$. The drawn observations are of the form $\boldsymbol{X}_{j^i}^{(k^i)}$ for some $k^i = 1, 2, j^i = 1, \ldots, T$, and $i = 1, 2$. Then, $\boldsymbol{X}_{j^i}^{(k^i)}$ is taken as the first element of the pseudo-series $\overline{\boldsymbol{X}}_t^{(i)*}$, i.e., $\overline{\boldsymbol{X}}_1^{(i)*} = \boldsymbol{X}_{j^i}^{(k^i)}$, for $i = 1, 2$.

Step 3. Once obtained $\overline{\boldsymbol{X}}_l^{(i)*} = \boldsymbol{X}_{j^i}^{(k^i)}$, for $l < T$ and $i = 1, 2$, the next bootstrap replication $\overline{\boldsymbol{X}}_{l+1}^{(i)*}$ is defined as $\boldsymbol{X}_{j^i+1}^{(k^i)}$ with probability $1 - p$, and drawn from $\widetilde{\boldsymbol{X}}_t$ with probability p. When $j^i = T$, the selected observation is $\boldsymbol{X}_1^{(2)}$ if $k^i = 1$ and $\boldsymbol{X}_1^{(1)}$ if $k^i = 2$.

Step 4. Repeat Step 3 until the pseudo-series $\overline{\boldsymbol{X}}_t^{(1)*}$ and $\overline{\boldsymbol{X}}_t^{(2)*}$ contain T observations. Based on the pseudo-series $\overline{\boldsymbol{X}}_t^{(1)*}$ and $\overline{\boldsymbol{X}}_t^{(2)*}$, compute the bootstrap version $\widehat{d}_{QCD}^*$ of $\widehat{d}_{QCD}$.

Step 5. Repeat B times Steps 2–4 to obtain $\widehat{d}_{QCD}^{(1)*}, \ldots, \widehat{d}_{QCD}^{(B)*}$.

Step 6. Given a significance level α, compute the quantile of order $1 - \alpha$, $q_{1-\alpha}^*$, based on the set $\left\{\widehat{d}_{QCD}^{(1)*}, \ldots, \widehat{d}_{QCD}^{(B)*}\right\}$. Then, the decision rule consists of rejecting H_0 if $\hat{d}_{QCD}\left(\boldsymbol{X}_t^{(1)}, \boldsymbol{X}_t^{(2)}\right) > q_{1-\alpha}^*$.

It is worth remarking that, likewise MBB procedure, a proper approximation of the null distribution of $\widehat{d}_{QCD}$ is also ensured here due to consider the pooled time series $\widetilde{\boldsymbol{X}_t}$ in the generating mechanism.

From now on, we will refer to the test presented in this section as SB.

5. Simulation study

In this section, we carry out a simulation study conducted to assess the performance with finite samples of the testing procedures presented in Sections 3 and 4. After describing the simulation mechanism, the main results are discussed.

5.1. Experimental design

The behavior of the testing methods was examined with pairs of MTS realizations, $\overline{\boldsymbol{X}}_t^{(1)} = \left\{\boldsymbol{X}_1^{(1)}, \ldots, \boldsymbol{X}_T^{(1)}\right\}$ and $\overline{\boldsymbol{X}}_t^{(2)} = \left\{\boldsymbol{X}_1^{(2)}, \ldots, \boldsymbol{X}_T^{(2)}\right\}$, simulated from bivariate processes selected to cover different dependence structures. Specifically, three types of generating models were considered, namely VARMA processes, nonlinear processes, and dynamic conditional correlation models. In all cases, the deviation from the null hypothesis of equal underlying processes was established in accordance with two criteria: (i) differences in the coefficients of the generating models (Scenarios 1, 2 and 3), and (ii) differences in the covariance structures or in the error distributions (Scenarios 4, 5 and 6). At each scenario, the degree of deviation between the simulated realizations is regulated by specific parameters (δ and γ) included in the formulation of the models. The specific generating models concerning each scenario are given below, taking into account that, unless otherwise stated, the error process $(\epsilon_{t,1}, \epsilon_{t,2})^\intercal$ consists of iid realizations following a bivariate Gaussian distribution.

Scenario 1. VAR(1) models given by

$$\begin{pmatrix} X_{t,1} \\ X_{t,2} \end{pmatrix} = \begin{pmatrix} 0.1+\delta & 0.1+\delta \\ 0.1+\delta & 0.1+\delta \end{pmatrix} \begin{pmatrix} X_{t-1,1} \\ X_{t-1,2} \end{pmatrix} + \begin{pmatrix} \epsilon_{t,1} \\ \epsilon_{t,2} \end{pmatrix}.$$

Scenario 2. TAR (threshold autoregressive) models given by

$$\begin{pmatrix} X_{t,1} \\ X_{t,2} \end{pmatrix} = \begin{pmatrix} (0.9-\delta)X_{t-1,2}I_{\{|X_{t-1,1}|\leqslant 1\}} + (\delta-0.3)X_{t-1,1}I_{\{|X_{t-1,1}|>1\}} \\ (0.9-\delta)X_{t-1,1}I_{\{|X_{t-1,2}|\leqslant 1\}} + (\delta-0.3)X_{t-1,2}I_{\{|X_{t-1,2}|>1\}} \end{pmatrix} + \begin{pmatrix} \epsilon_{t,1} \\ \epsilon_{t,2} \end{pmatrix}.$$

Scenario 3. GARCH models in the form $(X_{t,1}, X_{t,2})^\intercal = (\sigma_{t,1}\epsilon_{t,1}, \sigma_{t,2}\epsilon_{t,2})^\intercal$ with

$$\sigma_{t,1}^2 = 0.01 + 0.05X_{t-1,1}^2 + 0.94\sigma_{t-1,1}^2,$$

$$\sigma_{t,2}^2 = 0.5 + 0.2X_{t-1,2}^2 + 0.5\sigma_{t-1,2}^2,$$

$$\begin{pmatrix} \epsilon_{t,1} \\ \epsilon_{t,2} \end{pmatrix} \sim N\left[\begin{pmatrix} 0 \\ 0 \end{pmatrix}, \begin{pmatrix} 1 & \rho_t \\ \rho_t & 1 \end{pmatrix}\right],$$

where the correlation between the standardized shocks is given by $\rho_t = 0.9 - \delta$.

In Scenarios 1–3, $\overline{\boldsymbol{X}}_t^{(1)}$ is always generated by taking $\delta = 0$, while $\overline{\boldsymbol{X}}_t^{(2)}$ is generated using different values of δ, thus allowing to obtain simulation schemes under the null, when $\delta = 0$ also for $\overline{\boldsymbol{X}}_t^{(2)}$, and under the alternative otherwise.

Scenario 4. Models in Scenario 1 with $\delta = 0$ for both realizations and covariance matrix of the error process in the form $\begin{pmatrix} 1 & \gamma \\ \gamma & 1 \end{pmatrix}$.

Scenario 5. Models in Scenario 2 with $\delta = 0$ for both realizations and different error distributions: a zero-mean Gaussian distribution for $\overline{\boldsymbol{X}}_t^{(1)}$ and a multivariate t distribution with γ degrees of freedom for $\overline{\boldsymbol{X}}_t^{(2)}$.

Scenario 6. Models in Scenario 3 with $\delta = 0$ for both realizations and different error distributions: a zero-mean Gaussian distribution for $\overline{\boldsymbol{X}}_t^{(1)}$ and a multivariate t distribution with γ degrees of freedom for $\overline{\boldsymbol{X}}_t^{(2)}$.

In Scenarios 4–6, the deviation degree is governed by γ. In Scenario 4, $\overline{\boldsymbol{X}}_t^{(1)}$ is always generated with $\gamma = 0$, while $\overline{\boldsymbol{X}}_t^{(2)}$ comes from taking $\gamma = 0$ or $\gamma \neq 0$ depending on whether the null or alternative is respectively required. Since the t distribution converges to a standard normal distribution as the number of degrees of freedom tends to infinity, the null hypothesis in Scenarios 5 and 6 corresponds to an arbitrarily large value of γ ($\gamma = 10^7$), while the alternative is reached using small values of this parameter.

Note that, unlike Scenarios 1 and 2, Scenario 3 considers realizations with different covariance structure for the error vectors. Therefore, Scenario 6 is constructed in a different way than Scenarios 4 and 5.

Before examining the behaviour of the testing methods in the described scenarios, as a preliminary step, we carried out a graphical inspection of the quality of the approximations under the null provided by the different approaches. To that aim, we considered pairs of realizations of length $T = 200$ coming from the VAR(1) process in Scenario 1 with $\delta = 0$. In this setup, the true finite sample density of the test statistic $\widehat{d}^2_{QCD}$ was approximated via Monte Carlo and compared with the asymptotic density in (16) and with nonparametric density estimates based on 500 bootstrap replicates generated with the FDB, MBB and SB techniques. All of these densities are shown in Fig. 1.

It is clear from Fig. 1 that, whereas the bootstrap approaches provide a reliable estimation of the underlying density, the asymptotic distribution yields a very poor approximation. The same graphical inspection was also carried out in other scenarios considering moderate values for the series length and similar conclusions were reached. In addition, the computation times associated with the bootstrap methods are far below the ones for the asymptotic distribution. Specifically, computation of the densities in Fig. 1 took approximately 3.85, 1.58 and 1.64 min for the procedures FDB, MBB and SB, respectively, and 150.19 min in the case of the asymptotic distribution. Based on these arguments, and although the asymptotic distribution of $\widehat{d}_{QCD}$ could be useful for several purposes, we decided to eliminate the asymptotic test from the simulation study.

To assess empirically the size and power behavior of the different bootstrap methods, 200 replications of pairs of realizations $\overline{\boldsymbol{X}}_t^{(1)}$ and $\overline{\boldsymbol{X}}_t^{(2)}$ coming from the processes at each scenario were obtained. Realizations $\overline{\boldsymbol{X}}_t^{(2)}$ were generated according to the specific values of δ and γ given in Table 1.

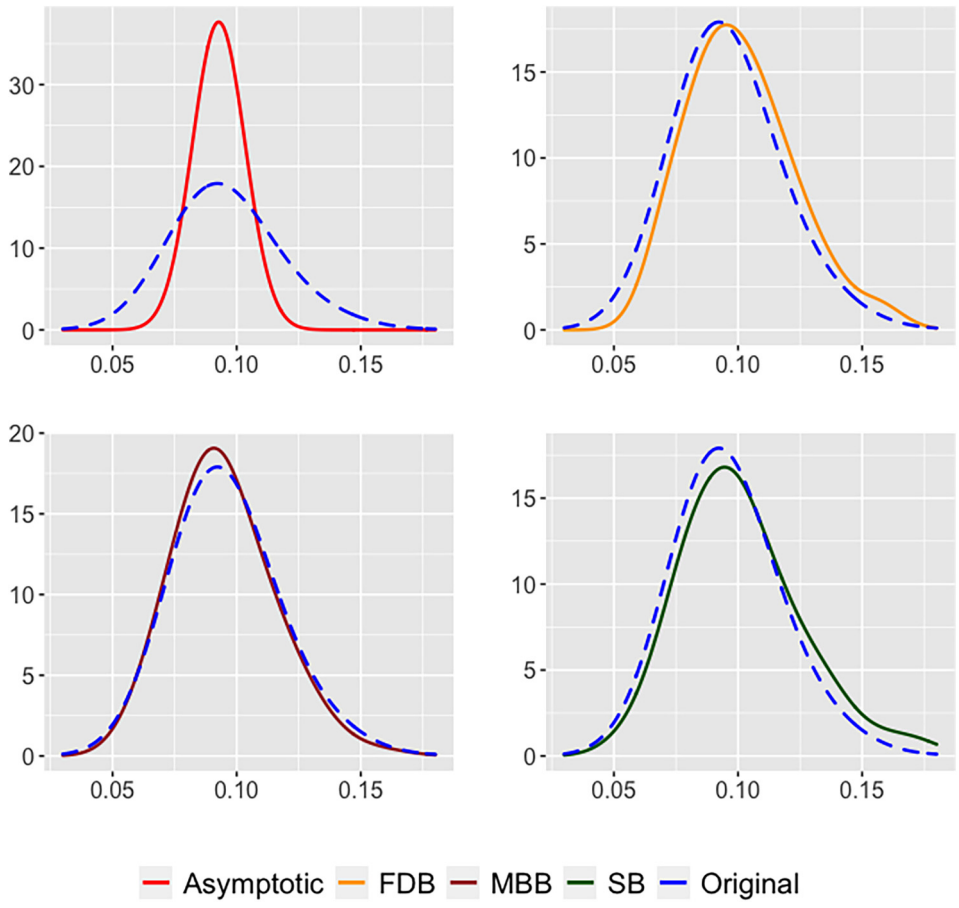

Fig. 1. Comparison between the true finite sample density of $\widehat{d}^2_{QCD}$ under the null in Scenario 1 ($T = 200$) and the approximations provided by its asymptotic distribution (top left) and the bootstrap methods FDB (top right), MBB (bottom left) and SB (bottom right).

At each trial, $B = 200$ bootstrap replicates were considered to approximate the distribution of the test statistic under the null hypothesis. In all cases, we selected the bandwidth $h_T = T^{-1/3}$ to compute $\widehat{d}_{QCD}$ and its bootstrap replicates. This choice ensures the consistency of the smoothed CCR-periodogram as an estimate of QCD (Theorem S4.1 in [31]) and the asymptotic validity of the FDB method (Assumption 4 in [26]). As for the two remaining methods, we chose $b = T^{1/3}$ and $p = T^{-1/3}$ for the block size in MBB and the probability in SB, respectively, since both values led to the best overall behavior of both procedures in our numerical experiments. Note that these choices are also consistent with the related literature. For instance, [41] addressed the issue of selecting b in the context of bias and variance bootstrap estimation, concluding that the optimal block size is of order $T^{1/3}$. On the other hand, since the mean block size in SB corresponds to $1/p$, it is reasonable to select p of order $T^{-1/3}$.

Simulations were carried out for different values of T. Our results showed that the three bootstrap procedures exhibit relatively high power when low to moderate sample sizes are used. However, larger samples sizes are necessary to reach a reasonable approximation of the nominal level. For this reason, the results included in next section correspond to $T \in \{500, 1000\}$, in the case of the null hypothesis, and $T \in \{100, 200, 300\}$, in the case of the alternative hypothesis. In all cases, the results were obtained for a significance level $\alpha = 0.05$.

5.2. Results and discussion

The results under the null hypothesis are summarized in Table 2, where the simulated rejection probabilities of the proposed bootstrap tests are displayed.

Table 2 clearly shows that the three bootstrap techniques exhibit different behaviors under the null hypothesis. The frequency domain-based test FDB is rather conservative when $T = 500$, providing rejection rates substantially lower than the theoretical ones. However, when increasing the value of the series length, the rejection levels of this test get close to 0.05. The MBB method provides rejection probabilities greater than expected for both values of T. In fact, the deviation from the theoretical significance level is more marked when $T = 1000$, particularly for Scenarios 3 and 5. The remaining technique SB seems to adjust the significance level quite well in all the analysed scenarios, which makes this test the most accurate one in terms of size approximation.

The estimated rejection probabilities under the set of considered alternative hypotheses are provided in Table 3, for Scenarios 1, 2 and 3, and in Table 4, for Scenarios 4, 5 and 6.

In all cases, the three bootstrap procedures lead to greater rejection rates when increasing the series length and the deviation from the null hypothesis, thus showing a reasonable behavior. The MBB method attains the largest rates except for Scenario 6, where this technique exhibits poor efficacy. It is particularly remarkable the instability showed by MBB in this scenario for $T = 300$ and $\gamma = 1/3$, where the method behaves totally unexpectedly. The good performance of MBB in terms of power was expected, since it showed rejection probabilities larger than the significance level under the null (see Table 2). The remaining procedures FDB and SB exhibit a very similar overall behavior. In fact, their rejection rates are very close to each other in Scenarios 1, 2, 3 and 4. On the other hand, the approach based on the stationary bootstrap SB attains higher power in Scenario 5, whereas the method FDB outperforms its counterpart in Scenario 6. In fact, FDB is the best performing approach in this scenario.

Table 1
Deviation parameters used to generate the second realization at each simulation scenario. Parameter values leading to the null hypothesis are indicated by adding (null).

Scenario	Parameter δ	Scenario	Parameter γ
1	0 (null), 0.1, 0.2, 0.3	4	0 (null), 0.3, 0.6, 0.9
2	0 (null), 0.2, 0.4, 0.6	5	10^7 (null), 3, 2, 1
3	0 (null), 0.4, 0.8, 1.2	6	10^7 (null), 1, 2/3, 1/3

Table 2
Simulated rejection probabilities under the null hypothesis for $\alpha = 0.05$.

		Scenario					
T	Method	1	2	3	4	5	6
500	FDB	0.025	0.020	0.035	0.020	0.020	0.030
	MBB	0.080	0.070	0.080	0.075	0.075	0.060
	SB	0.055	0.055	0.050	0.030	0.045	0.050
1000	FDB	0.060	0.030	0.060	0.045	0.040	0.040
	MBB	0.070	0.095	0.130	0.095	0.125	0.065
	SB	0.040	0.060	0.060	0.040	0.055	0.045

Table 3
Simulated rejection probabilities of the bootstrap tests under several alternative hypotheses determined by the deviation parameter δ in Scenarios 1, 2 and 3.

		Scenario 1			Scenario 2			Scenario 3		
		δ			δ			δ		
T	Method	0.1	0.2	0.3	0.2	0.4	0.6	0.4	0.8	1.2
100	FDB	0.060	0.395	0.905	0.340	0.695	0.950	0.030	0.150	0.895
	MBB	0.160	0.575	0.980	0.540	0.775	0.990	0.080	0.395	0.950
	SB	0.100	0.465	0.960	0.325	0.690	0.910	0.055	0.230	0.870
200	FDB	0.060	0.610	0.990	0.595	0.875	0.985	0.050	0.505	0.965
	MBB	0.185	0.790	0.995	0.780	0.925	1	0.185	0.725	1
	SB	0.095	0.695	0.990	0.625	0.885	0.985	0.080	0.455	0.965
300	FDB	0.115	0.730	1	0.765	0.965	1	0.135	0.730	1
	MBB	0.225	0.835	1	0.885	0.990	1	0.255	0.840	1
	SB	0.130	0.770	1	0.805	0.955	1	0.155	0.695	1

Table 4
Simulated rejection probabilities of the bootstrap tests under several alternative hypotheses determined by the deviation parameter γ in Scenarios 4, 5 and 6.

		Scenario 4			Scenario 5			Scenario 6		
		γ			γ			γ		
T	Method	0.3	0.6	0.9	3	2	1	1	2/3	1/3
100	FDB	0.080	0.365	0.910	0.115	0.390	0.830	0.085	0.195	0.360
	MBB	0.200	0.670	0.970	0.220	0.545	0.900	0.090	0.140	0.195
	SB	0.075	0.400	0.905	0.190	0.510	0.905	0.085	0.175	0.280
200	FDB	0.095	0.550	0.990	0.215	0.485	0.915	0.275	0.480	0.895
	MBB	0.245	0.845	1	0.435	0.675	0.965	0.190	0.310	0.355
	SB	0.100	0.635	0.995	0.335	0.610	0.995	0.210	0.345	0.765
300	FDB	0.225	0.850	1	0.220	0.565	1	0.625	0.865	0.995
	MBB	0.365	0.955	1	0.450	0.770	1	0.415	0.610	0.250
	SB	0.160	0.840	1	0.375	0.730	1	0.470	0.675	0.980

In summary, MBB shows the best performance in terms of power but an overrejecting behavior in terms of size. On the contrary, FDB and SB display worse effectiveness under the alternative hypothesis but they respect the nominal level under the null hypothesis. In particular, SB achieves rejection rates very close to the significance level. Therefore, this technique could be said to exhibit the best overall behavior according to both size and power.

6. A case study. Did the dotcom bubble change the global market behaviour?

In this section, the proposed bootstrap procedures are used to check whether the well-known dotcom bubble crash caused a permanent effect on the behaviour of financial markets worldwide. After providing some background on the dotcom bubble crash and presenting the considered dataset, the bootstrap tests are applied and the main conclusions stated. We want to remark that the following analysis is not aimed at giving financial advice, but at showing how the proposed tests can be useful for deriving economical implications.

6.1. The dotcom bubble crash

Historically, the dotcom bubble was a rapid rise in U.S. technology stock equity valuations exacerbated by investments in Internet-based companies during the bull market in the late 1990s. The value of equity markets grew substantially during this period, with the Nasdaq index rising from under 1000 to more than 5000 between the years 1995 and 2000. Things started to change in 2000, and the bubble burst between 2001 and 2002 with equities entering a bear market. The crash that followed saw the Nasdaq index tumble from a peak of 5048.62 on March 10, 2000, to 1139.90 on October 4, 2002, a 76.81% fall. By the end of 2001, most dotcom stocks went bust.

The dotcom bubble grew out of a combination of the presence of speculative or fad-based investing, the abundance of venture capital funding for startups, and the failure of dotcoms to turn a profit. Investors poured money into Internet startups during the 1990s hoping they would one day become profitable. Many investors and venture capitalists abandoned a cautious approach for fear of not being able to cash in on the growing use of the Internet. In the year 1999, 39 of all venture capital investments were going to Internet companies. That year, most of the 457 initial public offerings (IPOs) were related to Internet companies, followed by 91 in the first quarter of 2000 alone. As it is stated in Porras [42]: "There were many contributing factors to the dot-com bust, but overall, the key reason was the high growth expectations that never materialized.

The long-term potential of the sector overshadowed the short-term viability of specific companies". Companies that famously survived the bubble include Amazon, eBay, and Priceline.

It is worth remarking that, although the dotcom bubble took place originally in the United States, the global economy was substantially affected by this phenomenon. For instance, Kohn and Pereira [43] showed that European and US financial markets exhibited very high correlation during the dotcom bubble, thus confirming the presence of spillover effects between them. Chen and Poon [44] found that the dotcom bubble tremendously affected several Asian stock market indexes and some indexes pertaining to the developed world. Specifically, investors in these countries showed a much less willingness to put money into the market due to the dotcom burst, this phenomenon lasting approximately six months. In summary, the dotcom bubble produced a severe effect over the whole global economy.

Concerning the time period of the dotcom bubble, the majority of authors consider the dotcom bubble to take place in the period 1996–2000 [45]. In addition, it is assumed that the bubble burst period was between 2000 and 2002, since, as stated before, the Nasdaq index fell by 76.81% in October 4, 2002.

6.2. The considered data

To analyse the effects of the dotcom bubble in the global economy, we considered three well-known stock market indexes, which are briefly described below.

- **S&P 500**. This index is comprised of 505 common stocks issued by 500 large-cap companies and traded on stock exchanges in the United States. The S&P 500 gives weights to the companies according to their market capitalization.
- **FTSE 100**. This market index includes the 100 companies listed in the London Stock Exchange with the highest market capitalization. It is also a weighted index with weights depending on the market capitalization of the different firms.
- **Nikkei 225**. This index is a price-weighted, stock market index for the Tokyo Stock Exchange. It measures the performance of 225 large, publicly owned companies in Japan from a wide array of industry sectors.

We focus on the trivariate time series formed by the daily stock prices of the three mentioned indexes. The data were sourced from the finance section of the Yahoo website[1]. As our goal is to determine whether the dotcom bubble distorted the global market behaviour, we split this MTS into two separate periods: before and after the bubble burst. To this aim, we consider the periods from 1987 to 2002 and from 2003 to 2018, respectively. In addition, we only select dates corresponding to trading days for the three indexes and forming two periods of the same length. Based on these considerations, the first period covers the simultaneous trading days from January 2, 1987 to July 25, 2002, and the second period includes the simultaneous trading days from July 26, 2002 to December 28, 2018. In this way, each MTS is constituted by 3928 daily observations.

Two remarks concerning the considered data are given below.

Remark 4. Note that each of the selected periods corresponds to approximately 16 years of observations. We assume that a 16-year period is enough to capture the daily behaviour of the global economy concerning stock markets with a high degree of accuracy. In fact, other works have considered substantially shorter daily series to perform statistical analyses [46–48]. In addition, as we are studying the effect of the dotcom bubble burst occurring in 2000–2002, it would not be possible to choose a much longer interval than 16 years for the second period.

Remark 5. The selected multivariate time series involves the most well-known indexes of the American, European and Asian continents, whose economies were affected by the dotcom bubble crash to some extent as stated in Section 6.1. Therefore, it is reasonable to assume that the considered MTS is a good representative of the global markets and a suitable choice to analyse the impact of the dotcom bubble in the worldwide economy.

Fig. 2 shows the closing prices of the three stock indexes from January 2, 1987 to December 28, 2018. The vertical line at each panel accounts for the end of the dotcom bubble burst, splitting each series in the two considered periods. The three indexes indicate a bull market during the years preceding 2000, followed by a bear market after 2000, thus corroborating the correlation between the American, European and Asian stock markets during the dotcom bubble and the subsequent burst.

Since the series of closing prices are not stationary in mean, we proceed to take the first difference of the natural logarithm of the original values, thus obtaining series of so-called daily returns, which are depicted in Fig. 3. The new series exhibit common characteristics of financial time series, so-called "stylized facts", as heavy tails, volatility clustering and leverage effects. It is worth emphasizing that the distance d_{QCD} has proven specially useful when dealing with this kind of series in some contexts as clustering [10], outlier detection [49] and classification [50].

Two MTS are constructed by considering simultaneously the three UTS in Fig. 3 before and after the dotcom bubble crash (vertical line). Firstly, we check if both MTS are independent, since this assumption is required by the three bootstrap procedures. Note that, as we are considering two disjoint periods from the same MTS, it suffices to show that the original series is serially independent. Hence, we focus on testing

$$H_0^{ij} : \rho_{ij}(l) = 0 \quad \text{against} \quad H_1^{ij} : \rho_{ij}(l) \neq 0, \tag{24}$$

[1] https://es.finance.yahoo.com

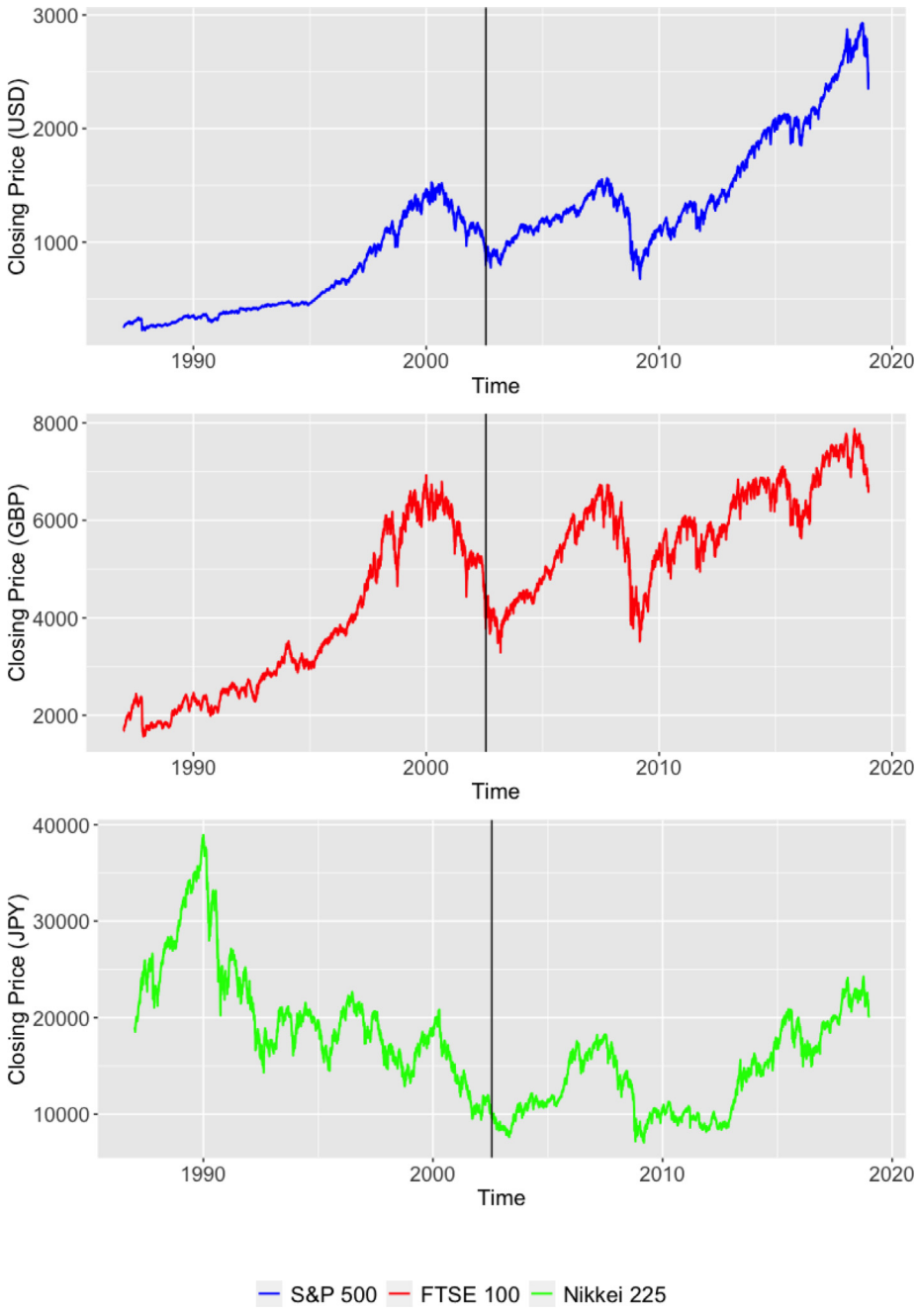

Fig. 2. Daily closing prices of the S&P 500 (top panel), FTSE 100 (middle panel) and Nikkei 225 (bottom panel) stock market indexes from January 2, 1987 to December 28, 2018. The vertical line indicates the end of the dotcom bubble burst.

for $i, j \in \{1, 2, 3\}$, where $\rho_{ii}(l) = Corr(X_{t,i}, X_{t+l,i})$ is the autocorrelation at lag l for the i-th component of the underlying process, and $\rho_{ij}(l) = Corr(X_{t,i}, X_{t+l,j}), i \neq j$, is the cross-correlation at lag l between the i-th and the j-th components. The tests in (24) were executed by considering the well-known sample versions of the auto and cross-correlations along with their corresponding asymptotic distributions under the null hypothesis. We selected the values of $l \in \{20, 100, 200\}$ to summarize the serial dependence structure of the process for moderate to large values of the lag. Table 5 contains the corresponding p-values.

Most of p-values in Table 5 indicate that the null hypothesis is not rejected at a significance level $\alpha = 0.05$. Only 3 p-values in Table 5 are below 0.05, but this could be due to the fact that we are performing several tests simultaneously. In fact, if we compute the corresponding adjusted p-values by means of classical methods as Bonferroni's, Holm's or Hommel's, all the

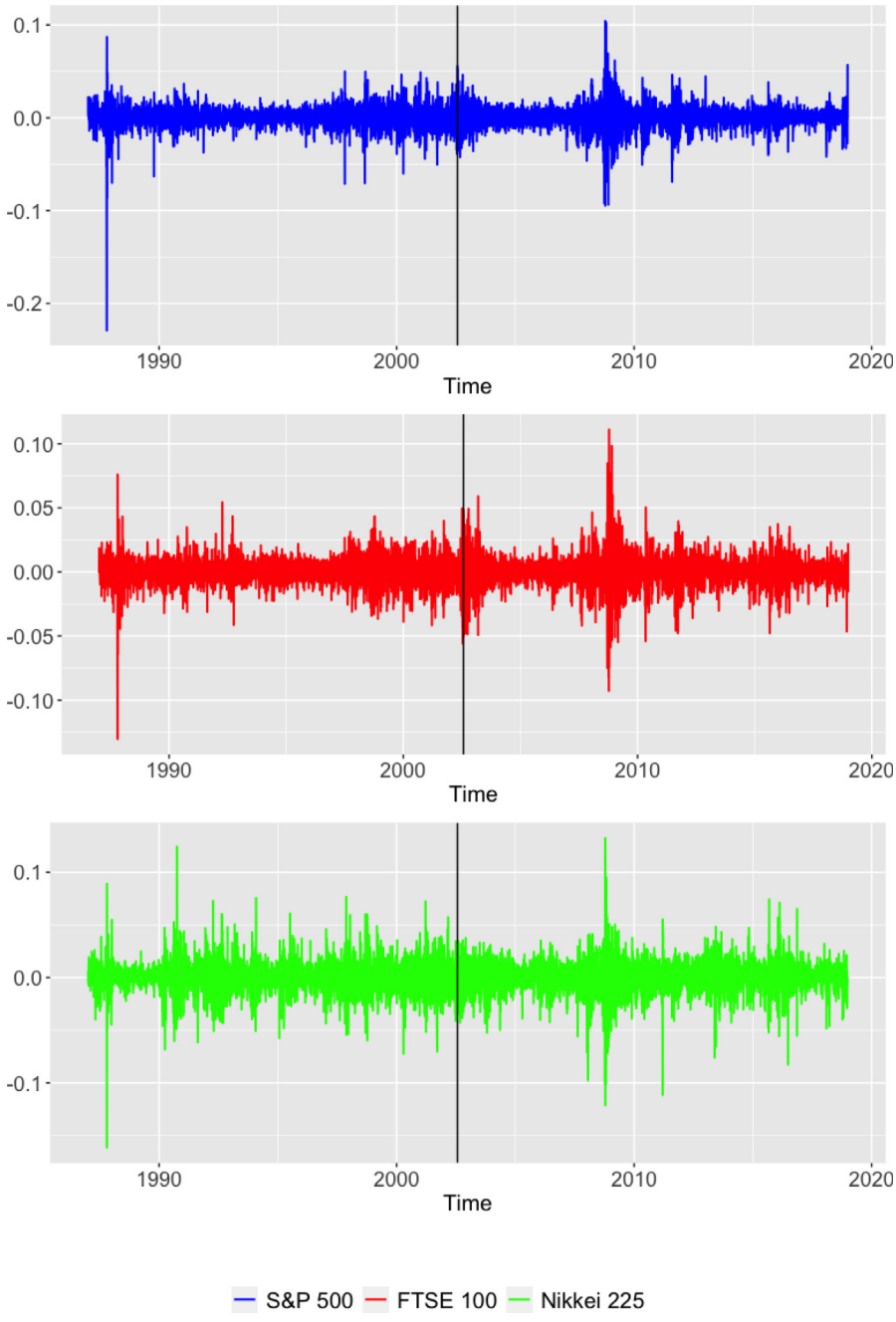

Fig. 3. Daily returns of the S&P 500 (top panel), FTSE 100 (middle panel) and Nikkei 225 (bottom panel) stock market indexes from January 2, 1987 to December 28, 2018. The vertical line indicates the end of the dotcom bubble burst.

new quantities are far greater than 0.05, and take the value of 1 in many cases. Therefore, we cannot reject the null hypothesis in any setting.

It is worth highlighting that similar results are obtained when all values of l are selected to be greater than 20 (although the corresponding p-values are not shown in the manuscript for the sake of simplicity). Note that the previous analyses do not guarantee independence between the last 20 observations of the first series and the first 20 observations of the second series. In fact, some amount of dependence exists between those two periods, but this is a minor issue because we are dealing with series of approximately 4000 observations. Therefore, independence can be assumed between both trivariate series in Fig. 3.

Table 5
For a given lag l, the entry associated with the i-th row and the j-th column of the corresponding subtable provides the p-value for the (ij)-th test in (24).

$l = 20$			$l = 100$			$l = 200$		
0.100	0.047	0.278	0.335	0.040	0.715	0.411	0.833	0.376
0.079	0.385	0.185	0.900	0.985	0.011	0.138	0.885	0.411
0.466	0.566	0.759	0.357	0.057	0.368	0.563	0.995	0.115

After verifying the assumption of independence, the equality of generating processes of both MTS was checked by using the bootstrap tests proposed throughout the manuscript based on $B = 500$ boostrap replicates.

6.3. Results

The p-values obtained by means of the methods FDB, MBB and SB were all 0. Therefore, the three bootstrap techniques indicate rejection of the null hypothesis at any reasonable significance level. This suggests that the whole MTS exhibits a different dependence structure at each of the considered periods. A direct implication of this fact could be that the dotcom bubble crash in the early 2000s provoked a permanent change in the behavior of the global economy.

Note that the methodology presented here can be applied to any pair of financial MTS created by splitting a longer MTS. This way, we are providing a procedure of broad applicability, since it is not uncommon in Economics to study the impact of pivotal occurrences (e.g., crashes, wars, election of a new president...) by analysing the market behaviour before and after the event. Indeed, given the high ability of the distance d_{QCD} to discriminate between dependence patterns of financial time series, we encourage researchers and practitioners in the field of Finance to consider the techniques presented in this manuscript.

7. Conclusions

In this work, we addressed the problem of testing the equality of two multivariate stochastic processes in terms of dependence structures. For that purpose, we first defined a distance measure between multivariate processes based on comparing their quantile cross-spectral densities, called d_{QCD}. Then, four tests considering a proper estimate of this dissimilarity ($\widehat{d}_{QCD}$) were proposed.

The first test uses the asymptotic distribution of $\widehat{d}_{QCD}$, which was established from standard results on complex random variables and Theorem S4.1 in [31]. Derivation of this asymptotic distribution is valuable in its own right, since $\widehat{d}_{QCD}$ has been successfully used to perform several MTS data mining tasks as clustering [10], classification [50] or outlier detection [49]. However, the slow convergence to the limit distribution, together with the significant amount of noise generated in the estimation of the asymptotic covariance, lead to a quite inaccurate test and rather useless from a practical point of view. The poor performance of the asymptotic test motivates the construction of alternative procedures capable of better approximating the underlying finite sample distribution of the test statistic. To this aim, we proposed to use several bootstrap procedures.

The second test (FDB) performs bootstrap in the frequency domain. Specifically, we formulated a general class of hypotheses introduced by [26] in terms of the distance d_{QCD}. The cornerstone of the procedure is an asymptotic property of the periodogram matrix of a multivariate series. The remaining two tests are extensions of the well-known moving blocks bootstrap (MBB) and stationary bootstrap (SB), respectively.

The three bootstrap techniques were evaluated by means of a simulation study including a wide variety of generating processes. Several settings under the null and alternative hypotheses were considered. The results indicate that the MBB test achieves the highest power but does not respect the nominal size. In contrast, FDB and SB show worse rejection rates under the alternative hypothesis but avoiding over-rejection under the null. Specifically, the test based on the stationary bootstrap SB exhibits the best overall performance with respect to both size and power.

In order to illustrate the usefulness of the proposed bootstrap tests, they were used to answer the question about whether or not the dotcom bubble burst of 2000s changed the behaviour of the global economy. To that aim, a trivariate MTS containing returns of stock market indexes was considered and split into two periods, before and after the crash. The tests were applied to check the equality of generating processes of the corresponding two MTS. In the three cases, the null hypothesis of equality got rejected, suggesting that the dotcom bubble crash provoked a permanent impact in the worldwide markets.

The approaches introduced in this manuscript suffer from two main limitations. First, the assumption of independence between both time series can be hard to fulfil in practice, since many real MTS exhibit some degree of cross-dependence or even spatial relationships. Second, when the dimension d is large, obtaining the bootstrap replicates of $\widehat{d}_{QCD}$ becomes computationally intensive, making the corresponding tests quite slow. In this regard, future work could address the construction of efficient hypothesis tests under the general case of an arbitrary dependence relation between $\overline{\boldsymbol{X}}_t^{(1)}$ and $\overline{\boldsymbol{X}}_t^{(2)}$. In addition, the corresponding tests could be particularly adapted to deal with financial time series by considering the specific features of this type of objects, since the problem of testing for independence between two MTS frequently arises in the fields of Economics and Finance.

CRediT authorship contribution statement

Ángel López-Oriona: Conceptualization, Writing - review & editing, Methodology, Software, Visualization. **José A. Vilar:** Conceptualization, Supervision, Writing - review & editing, Project administration.

Declaration of Competing Interest

The authors declare that they have no known competing financial interests or personal relationships that could have appeared to influence the work reported in this paper.

Acknowledgments

The authors are grateful to the associate editor and to the anonymous referees for their comments and suggestions. This research has been supported by the Ministerio de Economía y Competitividad (MINECO) grants MTM2017-82724-R and PID2020-113578RB-100, the Xunta de Galicia (Grupos de Referencia Competitiva ED431C-2020-14), and the Centro de Investigación del Sistema Universitario de Galicia "CITIC" grant ED431G 2019/01; all of them through the European Regional Development Fund (ERDF). This work has received funding for open access charge by Universidade da Coruña/CISUG.

Appendix A. About the asymptotic validity of FDB

In Section 4.1, the test for equality of quantile cross-spectral densities was stated as a particular case of the general class of spectral hypotheses (17). In order to testing (17), Dette and Paparoditis [26] propose a general bootstrap procedure to approximate the distribution of the test statistic

$$S_T(\varphi) = \int_{-\pi}^{\pi} \|\varphi(\widehat{g}(\omega), \omega)\|^2 \, d\omega,$$

and establish the conditions to ensure its asymptotic validity (see Theorem 1). In our setting, we also adopt the test statistic $S_T(\varphi)$ for the specification of the function φ given in (21), which allows us to establish $S_T(\varphi)$ in terms of the QCD-distance since

$$\|\varphi(g_z(\omega), \omega)\| = d_{QCD,\omega}\left(\boldsymbol{X}_t^{(1)}, \boldsymbol{X}_t^{(2)}\right).$$

This way, the FDB procedure fits into the framework considered in [26] and involves the QCD-distance. In what follows, we are going to show that the set of assumptions required in Theorem 1 in [26] are fulfilled, thus concluding the asymptotic validity of the FDB algorithm. We first check the assumptions about the underlying stochastic process, the function φ, the kernel W and the bandwidth h_T. Finally, we verify the assumptions concerning the version of the estimate $\hat{g}(\omega)$ used to generate the bootstrap replicates.

Appendix B. Assumptions on the stochastic processes, the function φ, the kernel function and the bandwidth

Assumption 1 in [26] is related to the vector moving average representation of the multivariate stochastic process defining the hypotheses in (17). This assumption ensures the existence of the spectral density matrix $g(\omega)$. Throughout this manuscript, it is also assumed the existence of the quantile cross-spectral density matrices of the strictly stationary processes $\boldsymbol{X}_t^{(1)}$ and $\boldsymbol{X}_t^{(2)}$. This way, the existence of the spectral density matrices of the process $\boldsymbol{Z}_t$ in (19) is also guaranteed.

Assumption 2 in [26] comprises four conditions concerning the function φ in (17). Below we state these conditions sequentially and verify that they are appropriately met.

1. The function $\varphi(V, \omega)$ is holomorphic with respect to V and satisfies $\|\varphi(V^\intercal, -\omega)\| = \|\varphi(V, \omega)\|$.
   Note that $\varphi : D \times [-\pi, \pi] \to \mathbb{C}^{r^2d^2}$, with D an open subset of $\mathbb{C}^{2r^2d^2 \times 2r^2d^2}$ containing the spectral density matrices evaluated in $\omega \in [-\pi, \pi]$. For a spectral matrix $V = (v_{ij}) \in D$ and $\omega \in [-\pi, \pi]$, $\varphi(V, \omega) = \left(\varphi_{11}(V, \omega), \ldots, \varphi_{rd,rd}(V, \omega)\right)^\intercal$, with $\varphi_{ij}(V, \omega) = v_{ij} - v_{i+rd,j+rd}$, for $i, j = 1, \ldots, rd$.
   By virtue of Hartogs' Theorem, it suffices to show that each φ_{ij} is holomorphic with respect to each one of the variables v_{rs} in V independently. But this is clearly fulfilled since fixed $(i, j) \in \{1, \ldots rd\} \times \{1, \ldots, rd\}$, we have $\partial\varphi_{ij}/\partial v_{ij} = 1, \partial\varphi_{ij}/\partial v_{i+rd,j+rd} = -1$ and $\partial\varphi_{ij}/\partial v_{rs} = 0$ for all $(r, s) \neq (i, j)$.
   On the other hand, by definition we have

$$vec\left(g_z^{(1)}(\omega)^\intercal\right) - vec\left(g_z^{(2)}(\omega)^\intercal\right) = vec\left(g_z^{(1)}(\omega)\right) - vec\left(g_z^{(2)}(\omega)\right),$$

which, jointly with the QCD property $\overline{\mathfrak{f}_{j_1 j_2}(\omega, \tau, \tau')} = \mathfrak{f}_{j_1 j_2}(-\omega, \tau, \tau')$, for all $\omega \in \mathbb{R}, j_1, j_2 \in \{1, \ldots, d\}$ and $\tau, \tau' \in [0, 1]$, where $\overline{z}$ stands for the complex conjugate of $z \in \mathbb{C}$, allows to conclude the equality $\|\phi(V^\intercal, -\omega)\| = \|\phi(V, \omega)\|$.

2. The function $\varphi(V,\omega)$ and its first derivative with respect to $v = vec(V), D_V\varphi(V,\omega) = \partial\varphi(V,\omega)/\partial v$, are piecewise Lipschitz continuous in ω.
   Note that each of the coordinate functions $\varphi_{ij}(\cdot)$ can be expressed as

$$\varphi_{ij}(V,\omega) = F_1(\omega) - F_2(\omega),$$

where F_1 and F_2 define some QCD for fixed variables and probability levels concerning the processes $\boldsymbol{X}_t^{(1)}$ and $\boldsymbol{X}_t^{(2)}$, respectively. To show the Lipschitz continuity of φ_{ij}, it suffices to show the same property for F_k, and, in turn, for $p(\omega) = e^{-il\omega}, l \in \mathbb{Z}$, due to the definition of QCD in (3). The function $p(\omega)$ is indeed Lipschitz continuous. Taking $\omega_1, \omega_2 \in \mathbb{R}, \omega_1 \leqslant \omega_2$, we have

$$|e^{-il\omega_1} - e^{-il\omega_2}| = |\int_{\omega_1}^{\omega_2} -ile^{-il\omega}d\omega| \leqslant \int_{\omega_1}^{\omega_2} |-ile^{-il\omega}|d\omega = l^2(\omega_2 - \omega_1),$$

thus concluding that l^2 is the Lipschitz constant for the function $p(\omega)$.
The Lipschitz continuity of $D_V\phi(V,\omega)$ with respect to ω is obvious since the Jacobian matrix of φ taking into account the derivatives with respect to $v = vec(V)$ is a constant matrix formed by 0s and 1s, and so it does not depend on the value of ω.

3. There is a positive constant η such that, for all $\omega \in [-\pi,\pi]$, the ball $B_{\eta,\omega} = \left\{V \in \mathbb{C}^{2d^2r^2\times 2d^2r^2} : \|g(\omega) - V\| \leqslant \eta\right\}$ is contained in D and
   $\sup_{\omega\in[-\pi,\pi]}\sup_{V\in B_{\eta,\omega}}||\varphi(V,\omega)|| < \infty$.
   This result holds in view of the continuity of the function φ in $D = \mathbb{C}^{2d^2r^2\times 2d^2r^2} \times [-\pi,\pi]$, which is a compact set.
4. $\int_{-\pi}^{\pi} \|D_V\varphi(g(\omega),\omega)\|\, d\omega > 0$. Condition 4 holds because $D_V\varphi(g(\omega),\omega)$ is a real constant matrix with at least one element different from zero.

Assumption 3 refers to the kernel function W used to compute the smoothed CCR-periodograms in (6). Specifically, W is required to be a bounded, symmetric, Lipschitz continuous and non-negative kernel with compact support $[-\pi,\pi]$ and satisfying $\int_{-\pi}^{\pi} W(x)dx = 2\pi$. Throughout this manuscript this assumption was also supposed to hold and in fact the kernel functions used in the numerical experiments satisfied the previous conditions. In particular, the Epanechnikov kernel was considered in the simulation study of Section 5.

Assumption 4 concerns the bandwidth h_T employed for the spectral estimates. It is assumed that $h_T \to 0$ as $T \to \infty$ such that $h_T \sim T^{-b}$ for some $1/4 < b < 1/2$. In this way, the rate at which the bandwidth h_T is allowed to converge to 0 as $T \to \infty$ ensures that the bias in estimating $g(\omega)$ vanishes sufficiently fast without affecting the asymptotic distribution of the test statistic (18). In our analyses, we used $h_T = T^{-1/3}$ so that Assumption 4 is verified. It is worth noting that this bandwidth also fulfils the assumption of Theorem S4.1 in [31] concerning the existence of constants $\gamma > 0$ and $k \in \mathbb{N}$ such that $h_T = o\left(T^{-1/(2k+1)}\right)$ and $h_T T^{1-\gamma} \to \infty$ as $T \to \infty$.

Appendix C. Assumptions on the version of the estimate used to generate the bootstrap replicates

These assumptions are encompassed within the so-called Condition 1 (see Section 3 in [26]). Particularly, the three assumptions refer to the version of the non-parametric estimate $\hat{g}(\omega)$ in (18) employed in the generation of the bootstrap replicates. Note that, following Section 4.1, this estimate is constructed as

$$\hat{g}_z(\omega) = \begin{pmatrix} \hat{G}_z(\omega) & 0_{rd} \\ 0_{rd} & \hat{G}_z(\omega) \end{pmatrix},\ \omega \in [-\pi,\pi], \tag{25}$$

where $\hat{G}_z(\omega)$ is given in (23). Hence, we must verify that assumptions in Condition 1 are met for $\hat{g}_z$. Below we state the three assumptions and check their fulfillment.

1. $\hat{g}_z$ is Hermitian and non-negative definite.
   The Hermitian character of $\hat{g}_z$ is derived from the Hermitian character of $\hat{G}_z$, which is in turn obtained from the Hermitian character of the smoothed CCR-periodogram in (6). The reasoning concerning the non-negative definitess character is analogous.
2. $\hat{g}_z$ satisfies $\varphi(\hat{g}_z(\omega),\omega) = \mathbf{0}$ for almost all $\omega \in (-\pi,\pi]$.
   Note that $\varphi(\hat{g}_z(\omega),\omega) = vec\left(\hat{G}_z(\omega)\right) - vec\left(\hat{G}_z(\omega)\right) = \mathbf{0}$.
3. $\hat{g}_z(\omega)$ converges in probability to a limit $g^l(\omega)$. For almost $\omega \in (-\pi,\pi]$, the limit satisfies that

$$\begin{aligned}\Gamma_{\varphi,l}(\omega)\{g^l(\omega)^\intercal \otimes g^l(\omega)\} &= \Gamma_{\varphi}(\omega)\{g(\omega)^\intercal \otimes g(\omega)\},\\ \Gamma_{\varphi,l}(-\omega)^\intercal\{g^l(\omega)^\intercal \otimes g^l(\omega)\} &= \Gamma_{\varphi}(-\omega)^\intercal\{g(\omega)^\intercal \otimes g(\omega)\},\end{aligned} \tag{26}$$

where

$$\begin{aligned}\Gamma_{\varphi}(\omega) &= \overline{D_V\varphi(g(\omega),\omega)}D_V\varphi(g(\omega),\omega),\\ \Gamma_{\varphi,l}(\omega) &= \overline{D_V\varphi(g^l(\omega),\omega)}D_V\varphi\big(g^l(\omega),\omega\big).\end{aligned} \tag{27}$$

The convergence in probability of $\hat{g}_z(\omega)$ is clear from the convergence in probability of the smoothed periodogram as an estimate of the spectral density. In fact, the quantity $\hat{g}_z(\omega)$ converges in probability to the average spectral density of the processes $\boldsymbol{Z}_t^{(1)}$ and $\boldsymbol{Z}_t^{(2)}$.

To show (26), note that both $D_V\varphi(g(\omega),\omega)$ and $D_V\varphi\big(g^l(\omega),\omega\big)$ are the same constant matrix, i.e., they do not depend on V or ω. Therefore Γ_{φ} and $\Gamma_{\varphi,l}$ are also the same constant matrix.

References

[1] S. Aghabozorgi, A.S. Shirkhorshidi, T.Y. Wah, Time-series clustering–a decade review, Inform. Syst. 53 (2015) 16–38.
[2] A. Abanda, U. Mori, J.A. Lozano, A review on distance based time series classification, Data Min. Knowl. Disc. 33 (2) (2019) 378–412.
[3] A. Blázquez-García, A. Conde, U. Mori, J.A. Lozano, A review on outlier/anomaly detection in time series data, ACM Comput. Surveys (CSUR) 54 (3) (2021) 1–33.
[4] R.S. Tsay, Nonlinearity tests for time series, Biometrika 73 (2) (1986) 461–466.
[5] P. D'Urso, L. De Giovanni, R. Massari, Garch-based robust clustering of time series, Fuzzy Sets Syst. 305 (2016) 1–28.
[6] B. Lafuente-Rego, J.A. Vilar, Clustering of time series using quantile autocovariances, Advances in Data Analysis and Classification 10 (3) (2016) 391–415.
[7] R.J. Kate, Using dynamic time warping distances as features for improved time series classification, Data Min. Knowl. Disc. 30 (2) (2016) 283–312.
[8] J. Lines, S. Taylor, A. Bagnall, Time series classification with hive-cote: The hierarchical vote collective of transformation-based ensembles, ACM Trans. Knowl. Discovery Data 12 (5).
[9] E.A. Maharaj, A.M. Alonso, Discriminant analysis of multivariate time series: Application to diagnosis based on ecg signals, Computat. Stat. Data Anal. 70 (2014) 67–87.
[10] Á. López-Oriona, J.A. Vilar, Quantile cross-spectral density: A novel and effective tool for clustering multivariate time series, Expert Syst. Appl. 185 (2021) 115677.
[11] P. D'Urso, L.A. García-Escudero, L. De Giovanni, V. Vitale, A. Mayo-Iscar, Robust fuzzy clustering of time series based on b-splines, Int. J. Approximate Reasoning 136 (2021) 223–246.
[12] R. Cerqueti, M. Giacalone, R. Mattera, Model-based fuzzy time series clustering of conditional higher moments, Int. J. Approximate Reasoning 134 (2021) 34–52.
[13] A.M. Alonso, P. D'Urso, C. Gamboa, V. Guerrero, Cophenetic-based fuzzy clustering of time series by linear dependency, Int. J. Approximate Reasoning 137 (2021) 114–136.
[14] R. Cerqueti, P. D'Urso, L. De Giovanni, M. Giacalone, R. Mattera, Weighted score-driven fuzzy clustering of time series with a financial application, Expert Syst. Appl. 198 (2022) 116752.
[15] Y. Kakizawa, R.H. Shumway, M. Taniguchi, Discrimination and clustering for multivariate time series, J. Am. Stat. Assoc. 93 (441) (1998) 328–340.
[16] J. Caiado, N. Crato, D. Peña, A periodogram-based metric for time series classification, Comput. Stat. Data Anal. 50 (10) (2006) 2668–2684.
[17] E.A. Maharaj, P. D'Urso, Fuzzy clustering of time series in the frequency domain, Inf. Sci. 181 (7) (2011) 1187–1211.
[18] P. D'Urso, L. De Giovanni, R. Massari, R.L. D'Ecclesia, E.A. Maharaj, Cepstral-based clustering of financial time series, Expert Syst. Appl. 161 (2020) 113705.
[19] Á. López-Oriona, J.A. Vilar, P. D'Urso, Quantile-based fuzzy clustering of multivariate time series in the frequency domain, Fuzzy Sets Syst. 443 (2022) 115–154, from Learning to Modeling and Control.
[20] Á. López-Oriona, P. D'Urso, J.A. Vilar, B. Lafuente-Rego, Quantile-based fuzzy C-means clustering of multivariate time series: Robust techniques, Int. J. Approximate Reasoning 150 (2022) 55–82.
[21] Á. López-Oriona, P. D'Urso, J.A. Vilar, B. Lafuente-Rego, Spatial weighted robust clustering of multivariate time series based on quantile dependence with an application to mobility during covid-19 pandemic, IEEE Trans. Fuzzy Syst. 30 (9) (2022) 3990–4004.
[22] J. Swanepoel, J. Van Wyk, The comparision of two spectral density functions using the bootstrap, J. Stat. Comput. Simul. 24 (3–4) (1986) 271–282.
[23] J. Timmer, M. Lauk, W. Vach, C. Lücking, A test for a difference between spectral peak frequencies, Comput. Stat. Data Anal. 30 (1) (1999) 45–55.
[24] E.A. Maharaj, Comparison of non-stationary time series in the frequency domain, Computat. Stat. Data Anal. 40 (1) (2002) 131–141.
[25] K. Fokianos, A. Savvides, On comparing several spectral densities, Technometrics 50 (3) (2008) 317–331.
[26] H. Dette, E. Paparoditis, Bootstrapping frequency domain tests in multivariate time series with an application to comparing spectral densities, J. R. Stat. Soc.: Ser. B (Statistical Methodology) 71 (4) (2009) 831–857.
[27] P. Preuß, T. Hildebrandt, Comparing spectral densities of stationary time series with unequal sample sizes, Stat. Prob. Lett. 83 (4) (2013) 1174–1183.
[28] H. Dette, T. Kinsvater, M. Vetter, Testing non-parametric hypotheses for stationary processes by estimating minimal distances, J. Time Ser. Anal. 32 (5) (2011) 447–461.
[29] C. Jentsch, M. Pauly, Testing equality of spectral densities using randomization techniques, Bernoulli 21 (2) (2015) 697–739.
[30] M.R. Mahmoudi, M.H. Heydari, R. Roohi, A new method to compare the spectral densities of two independent periodically correlated time series, Math. Comput. Simul. 160 (2019) 103–110.
[31] J. Baruník, T. Kley, Quantile coherency: A general measure for dependence between cyclical economic variables, Econometr. J. 22 (2) (2019) 131–152.
[32] H.R. Kunsch, The jackknife and the bootstrap for general stationary observations, Annals Stat. (1989) 1217–1241.
[33] R.Y. Liu, K. Singh, et al, Moving blocks jackknife and bootstrap capture weak dependence, Exploring the limits of bootstrap 225 (1992) 248.
[34] D.N. Politis, J.P. Romano, The stationary bootstrap, J. Am. Stat. Assoc. 89 (428) (1994) 1303–1313.
[35] T. Kley, S. Volgushev, H. Dette, M. Hallin, Quantile spectral processes: Asymptotic analysis and inference, Bernoulli 22 (3) (2016) 1770–1807.
[36] A.M. Mathai, S.B. Provost, Quadratic forms in random variables: theory and applications, Dekker, 1992.
[37] P. Moschopoulos, W. Canada, The distribution function of a linear combination of chi-squares, Comput. Math. Appl. 10 (4–5) (1984) 383–386.
[38] H.-T. Ha, S.B. Provost, An accurate approximation to the distribution of a linear combination of non-central chi-square random variables, REVSTAT–Stat. J. 11 (3) (2013) 231–254.
[39] P.L. de Micheaux, M.P.L. de Micheaux, Package 'compquadform', CRAN Repository.
[40] P.J. Brockwell, R.A. Davis, Time series: theory and methods, Springer-Verlag, 1991.

[41] P. Hall, J.L. Horowitz, B.-Y. Jing, On blocking rules for the bootstrap with dependent data, Biometrika 82 (3) (1995) 561–574.
[42] E.R. Porras, Introduction to bubbles and contagion, Bubbles and Contagion in Financial Markets, vol. 1, Springer, 2016, pp. 1–30.
[43] M.-B.H. Kohn, P.L.V. Pereira, Speculative bubbles and contagion: Analysis of volatility's clusters during the dotcom bubble based on the dynamic conditional correlation model, Cogent Econ. Finance 5 (1) (2017) 1411453.
[44] S. Chen, S.-H. Poon, Modelling international stock market contagion using copula and risk appetite, Available at SSRN 1024288.
[45] J.J. Morris, P. Alam, Value relevance and the dot-com bubble of the 1990s, Q. Rev. Econ. Finance 52 (2) (2012) 243–255.
[46] P. D'Urso, C. Cappelli, D. Di Lallo, R. Massari, Clustering of financial time series, Physica A 392 (9) (2013) 2114–2129.
[47] F. Durante, R. Pappadà, N. Torelli, Clustering of financial time series in risky scenarios, Adv. Data Anal. Classif. 8 (4) (2014) 359–376.
[48] F. Lisi, Testing asymmetry in financial time series, Quant. Finance 7 (6) (2007) 687–696.
[49] Á. López-Oriona, J.A. Vilar, Outlier detection for multivariate time series: A functional data approach, Knowl.-Based Syst. 233 (2021) 107527.
[50] Á. López-Oriona, J.A. Vilar, F4: An all-purpose tool for multivariate time series classification, Mathematics 9 (23) (2021) 3051.